Dalton Transactions

View Online
Dynamic Article Links

Cite this: *Dalton Trans.*, 2011, **40**, 2588

www.rsc.org/dalton

PAPER

Coulombic inter-ligand repulsion effects on the Pt(II) coordination chemistry of oligocationic, ammonium-functionalized triarylphosphines†

Dennis J. M. Snelders,[a] Maxime A. Siegler,[b] Lars S. von Chrzanowski,[b] Anthony L. Spek,[b] Gerard van Koten[a] and Robertus J. M. Klein Gebbink*[a]

Received 26th August 2010, Accepted 26th November 2010
DOI: 10.1039/c0dt01105c

The Pt(II) coordination chemistry of oligocationic ammoniomethyl- and neutral aminomethyl-substituted triarylphosphines (L) is described. Complexes of the type $PtX_2(L)_2$ (X = Cl, I) have been isolated and characterized. For the hexa-*meta*-ammoniomethyl-substituted ligands $[\mathbf{1}]^{6+}$ and $[\mathbf{2}]^{6+}$, two ligands always occupy a *trans*-configuration with respect to each other in complexes of the type $PtX_2(L)_2$, while for the tri-*para*-ammoniomethyl-substituted ligand $[\mathbf{7}]^{3+}$, the *trans*/*cis* ratio is dependent on the ionic strength of the solution. This behaviour was not observed for the neutral aminomethyl-substituted ligands. In the crystal structure of *trans*-$[PtI_2(\mathbf{1})_2]I_{12}$, the geometrical parameters of the phosphine ligand $[\mathbf{1}]^{6+}$ are very similar to those found in the analogous complex of the benchmark ligand PPh_3, *i.e.* *trans*-$PtI_2(PPh_3)_2$, indicating that no significant increase in the steric congestion is present in the complex. Instead, the coordination chemistry of this class of phosphine ligands is dominated by repulsive Coulombic inter-ligand interactions.

1 Introduction

The use of additional supramolecular interactions between phosphine ligands coordinated to a metal centre is emerging as an important tool in the design of new ligand systems.[1] In particular, the construction of bidentate phosphine ligands, which self-assemble from monodentate phosphines *via* attractive noncovalent interactions, is a powerful concept.[2,3] Of special interest is the design of bidentate phosphine ligands that are exclusively *trans*-chelating.[4] The supramolecular interactions involved are in most cases hydrogen bonding or metal–ligand interactions.

Van Leeuwen *et al.*[5] reported on the use of Coulombic interactions to assemble triphenylphosphine derivatives. It was shown that the cationic and anionic moieties of two different phosphine ligands form ion pairs and that the resulting diphosphine ligand acts as a bidentate, *cis*- or *trans*-chelating ligand in various transition-metal complexes.

Hydrogen bonding, metal–ligand interactions or Coulombic attractive forces between opposite charges, as supramolecular interactions are all attractive in nature. However, in the case of Coulombic interactions, the combination of functional groups of the same charge should give rise to *repulsive* interactions between the phosphine ligands. Although several examples of phosphine ligands bearing anionic[6] as well as cationic[7] (Fig. 1) substituents exist, the number of ionic groups per phosphine functionality is usually limited to one, two or three. Ligands of this type have mainly been investigated to enhance the solubility of catalysts in polar or unconventional media and to enable their recycling, *e.g.* through an aqueous/organic biphasic setup.[8] Perhaps for these reasons, repulsive Coulombic interactions between phosphine ligands have only scarcely been described in the literature.[1a]

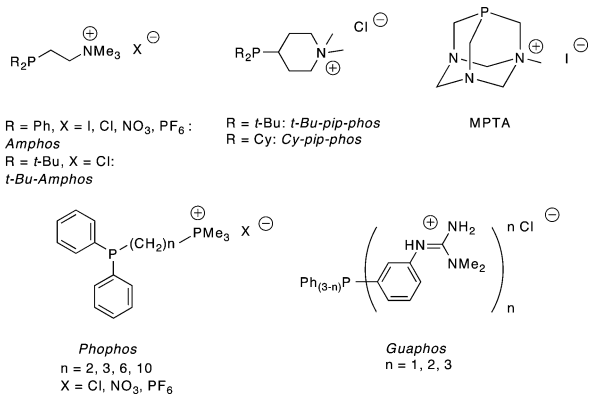

Fig. 1 Some known examples of cationic phosphine ligands.

The hexa-ammoniomethyl-functionalized *Dendriphos* ligands $[\mathbf{1}]^{6+}$ and $[\mathbf{2}]^{6+}$ (Fig. 2) were recently reported by us[9a] and the application of $[\mathbf{2}]Br_6$, as well as the higher generations of this class of ligands in the Pd-catalyzed Suzuki-Miyaura cross-coupling reaction, has been investigated.[9b–d] The high activity in the Suzuki-Miyaura

[a]*Organic Chemistry & Catalysis, Debye Institute for Nanomaterials Science, Faculty of Science, Utrecht University, Padualaan 8, 3584 CH Utrecht, The Netherlands. E-mail: r.j.m.kleingebbink@uu.nl; Fax: (+31)30-252-3615*
[b]*Crystal and Structural Chemistry, Bijvoet Center for Biomolecular Research, Faculty of Science, Utrecht University, Padualaan 8, 3584 CH Utrecht, The Netherlands*

† CCDC reference numbers 791148 and 791149. For crystallographic data in CIF or other electronic format see DOI: 10.1039/c0dt01105c

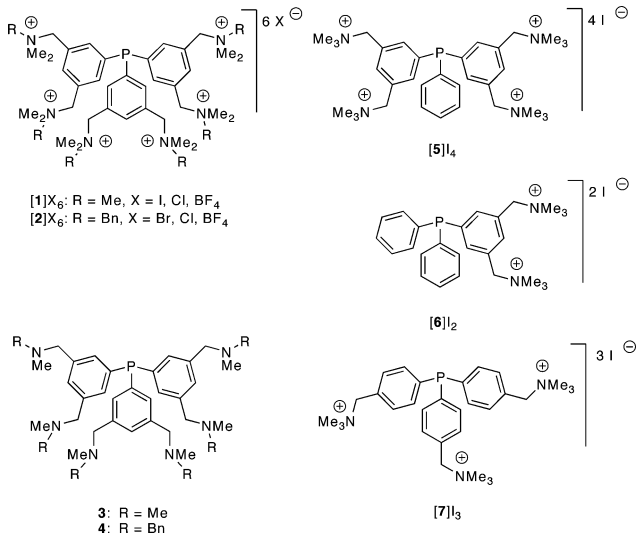

Fig. 2 The oligocationic ammoniomethyl- and neutral aminomethyl-substituted ligands considered in the present study.

reaction of catalytic systems employing these ligands is ascribed to a Coulombic repulsive interaction between neighbouring ligands, leading to a preferential formation of coordinatively unsaturated complexes. Next to the hexacationic *Dendriphos* ligands, di-, tri and tetra-ammoniomethyl functionalized $[\mathbf{5}]^{4+}$, $[\mathbf{6}]^{2+}$ and $[\mathbf{7}]^{3+}$ have been developed.[9d] Hexa-aminomethyl functionalized **3**[14] and **4**[9d] were designed as neutral, sterically similar analogues of $[\mathbf{1}]^{6+}$ and $[\mathbf{2}]^{6+}$. Here, we turn our attention to the reactivity of this series of oligocationic ligands, as well as their neutral analogues **3** and **4**, with respect to Pt(II) ions and present investigations concerning the role that repulsive Coulombic interactions play in their coordination behaviour.

2 Results

2.1 The reaction of hexacationic and neutral ligands with $PtCl_2$(cod).

Two equiv. of either the hexa-ammonium chloride ligand $[\mathbf{1}]Cl_6$ or $[\mathbf{2}]Cl_6$ were added to $PtCl_2$(cod) in MeOH–CH_2Cl_2 and stirred for 1 h at reflux temperature. Analysis of the products by ^{31}P-NMR in CD_3OD showed one singlet resonance in each case, at 24.5 ppm and 24.8 ppm, respectively, with ^{31}P–^{195}Pt coupling constants of 2655 and 2663 Hz (Table 1, entries 1 and 7). The magnitudes of these coupling constants are characteristic for *trans*-$PtCl_2L_2$ (L = tertiary phosphine) complexes.[10] No other peaks were observed, indicating that the complexes *trans*-$[PtCl_2L_2]Cl_{12}$ (**8a**: L = **1**; **8b**: L = **2**) were the only products of these reactions (Scheme 1). The complexes were isolated and fully characterized. ESI-MS spectra showed peaks corresponding to the ions $[PtL_2]Cl_{(14-n)}^{n+}$ (L = **1**, **2**; n = 3, 4. Table 2, entries 1, 2), which is consistent with the coordination of two phosphine ligands to the Pt centre. Ionization by the loss of multiple halide ions is generally observed for this type of oligocationic compound.[9a,11]

After the addition of 0.2 equiv. of free $[\mathbf{1}]Cl_6$ or $[\mathbf{2}]Cl_6$ to a solution in CD_3OD of *trans*-**8a** or *trans*-**8b**, respectively and heating to 65 °C, or after standing for 1 week in solution at room temperature, the only species observed by ^{31}P-NMR were *trans*-**8a–b**, indicating that these complexes do not undergo *trans–cis* isomerization, even in the presence of excess phosphine.[12] In order to investigate whether the *trans*-isomers are the kinetic products, or whether they are formed *via* thermal isomerization of the *cis*-isomers, the reactions of $[\mathbf{1}]Cl_6$ and $[\mathbf{2}]Cl_6$ with $PtCl_2$(cod) were performed at room temperature. The ^{31}P-NMR spectra of the products in CD_3OD now showed *trans*-**8a–b**, along with a second minor peak at 28.3 ppm ($^1J_{P,Pt}$ = 4436, in the case of $[\mathbf{1}]Cl_6$) and 28.2 ppm ($^1J_{P,Pt}$ = 4430, in the case of $[\mathbf{2}]Cl_6$). Upon heating the solutions to 65 °C, this peak completely disappeared and did

Table 1 ^{31}P-NMR spectral data for the products of the respective reactions of **1–4**, PPh_3 and P(4-$CF_3C_6H_4)_3$ with $PtCl_2$(cod)

					^{31}P-NMR		
Entry	L	L/Pt	Solvent	Product(s)	δ (ppm)	$^1J_{P,Pt}$ (Hz)	% obs.[a]
1	$[\mathbf{1}]Cl_6$	2	CD_3OD	*trans*-$[PtCl_2(\mathbf{1})_2]Cl_{12}$ (**8a**)	24.5	2655	100
2	$[\mathbf{1}]Cl_6$	2	D_2O	*trans*-$[PtCl_2(\mathbf{1})_2]Cl_{12}$ (**8a**)	23.9	2652	100
3	$[\mathbf{1}]Cl_6$	1	DMSO-d_6	$[PtCl_3(\mathbf{1})]Cl_5$	9.0	3946	100
4	$[\mathbf{1}]Cl_6$	2	DMSO-d_6	*trans*-$[PtCl_2(\mathbf{1})_2]Cl_{12}$ (**8a**)	23.5	2627	100
5	$[\mathbf{1}][BF_4]_6$	1	DMSO-d_6	*cis*-$[PtCl_2(DMSO)(\mathbf{1})][BF_4]_6$	16.9	3828	100
6	$[\mathbf{1}][BF_4]_6$	2	DMSO-d_6	*trans*-$[PtCl_2(\mathbf{1})_2][BF_4]_{12}$	23.7	2682	100
7	$[\mathbf{2}]Cl_6$	2	CD_3OD	*trans*-$[PtCl_2(\mathbf{2})_2]Cl_{12}$ (**8b**)	24.8	2663	100
8	$[\mathbf{2}]Cl_6$	1	DMSO-d_6	$[PtCl_3(\mathbf{2})]Cl_5$	8.2	3960	100
9	$[\mathbf{2}]Cl_6$	2	DMSO-d_6	*trans*-$[PtCl_2(\mathbf{2})_2]Cl_{12}$ (**8b**)	23.0	2642	100
10	$[\mathbf{2}][BF_4]_6$	1	DMSO-d_6	*cis*-$[PtCl_2(DMSO)(\mathbf{2})][BF_4]_6$	16.3	3818	100
11	$[\mathbf{2}][BF_4]_6$	2	DMSO-d_6	*trans*-$[PtCl_2(\mathbf{2})_2][BF_4]_{12}$	24.6	not obs.	100
12[b]	**3**	2	C_6D_6	*cis*-$PtCl_2(\mathbf{3})_2$ (**9a**)	14.7	3641	100
13	**4**	2	DMSO-d_6	*cis*-$PtCl_2(\mathbf{4})_2$ (**9b**)	15.4	3649	70
				trans-$PtCl_2(\mathbf{4})_2$ (**9b**)	21.0	2615	30
14[c]	PPh_3	1	DMSO-d_6	*cis*-$PtCl_2(PPh_3)_2$	14.9	3681	25
				trans-$PtCl_2(PPh_3)_2$	21.7	2626	5
				cis-$PtCl_2(DMSO)(PPh_3)$	17.6	3798	35
				$[NBu_4][PtCl_3PPh_3]$	7.2	3945	35
15	PPh_3	2	DMSO-d_6	*cis*-$PtCl_2(PPh_3)_2$	14.9	3681	100
16	P(4-$CF_3C_6H_4)_3$	2	DMSO-d_6	*cis*-$PtCl_2$(P(4-$CF_3C_6H_4)_3)_2$	14.9	3655	100

[a] Relative percentages. [b] Ref. 14 [c] Reaction performed in the presence of NBu_4Cl (6 equiv. with respect to PPh_3).

Table 2 The major ions observed by ESI-MS analysis of the selected complexes

Entry	Structure	Major ions observed	Calcd (*m*/*z*)	Found (*m*/*z*)
1[a]	$[PtCl_2(\mathbf{1})_2]Cl_{12}$ (**8a**)	$[Pt(\mathbf{1})_2]Cl_{11}^{3+}$	658.59	658.62
		$[Pt(\mathbf{1})_2]Cl_{10}^{4+}$	484.70	484.72
2[a,b]	$[PtCl_2(\mathbf{2})_2]Cl_{12}$ (**8b**)	$[Pt(\mathbf{2})_2]Cl_{11}^{3+}$	962.390	962.385
		$[Pt(\mathbf{2})_2]Cl_{10}^{4+}$	713.046	713.050
3[c]	$[PtCl_3(\mathbf{1})]Cl_5$	$[Pt(\mathbf{1})]Cl_6^{2+}$	551.18	551.22
4[c]	$[PtCl_3(\mathbf{2})]Cl_5$	$[Pt(\mathbf{2})]Cl_6^{2+}$	779.27	779.31
		$[Pt(\mathbf{2})]Cl_5^{3+}$	507.86	508.26
5[c]	$[PtCl_2(DMSO)(\mathbf{1})][BF_4]_6$	$[PtCl_2(DMSO)(\mathbf{1})][BF_4]_4^{2+}$	696.24	696.38
		$[PtCl_2(DMSO)(\mathbf{1})][BF_4]_3^{3+}$	435.16	435.24
6[c]	$[PtCl_2(DMSO)(\mathbf{2})][BF_4]_6$	$[PtCl_2(DMSO)(\mathbf{2})][BF_4]_4^{2+}$	924.38	924.47
		$[PtCl_2(DMSO)(\mathbf{2})][BF_4]_3^{3+}$	587.58	587.31
7[d]	$[PtCl_2(\mathbf{1})_2][BF_4]_{12}$	$[PtCl_2(\mathbf{1})_2][BF_4]_9^{3+}$	812.36	812.39
		$[PtCl_2(\mathbf{1})_2][BF_4]_8^{4+}$	587.52	587.53
8[c]	$[PtI_3(\mathbf{1})]I_5$	$[Pt(\mathbf{1})]I_6^{2+}$	825.49	825.58
		$[Pt(\mathbf{1})]I_5^{3+}$	508.03	508.07
		$[Pt(\mathbf{1})]I_4^{4+}$	349.30	349.32

[a] Prepared by the reaction of $PtCl_2$(cod) with two equiv. of [**1**]Cl_6 or [**2**]Cl_6, respectively, in MeOH–CH_2Cl_2. [b] High resolution measurement. [c] Prepared by the reaction of PtX_2(cod) with one equiv. [**1**]Cl_6, [**2**]Cl_6, [**1**]$[BF_4]_6$, [**2**]$[BF_4]_6$ (X = Cl) or [**1**]I_6 (X = I), respectively, in DMSO-d_6. [d] Prepared by the reaction of $[PtCl_2(DMSO)(\mathbf{1})][BF_4]_6$ with [**1**]$[BF_4]_6$ in DMSO-d_6.

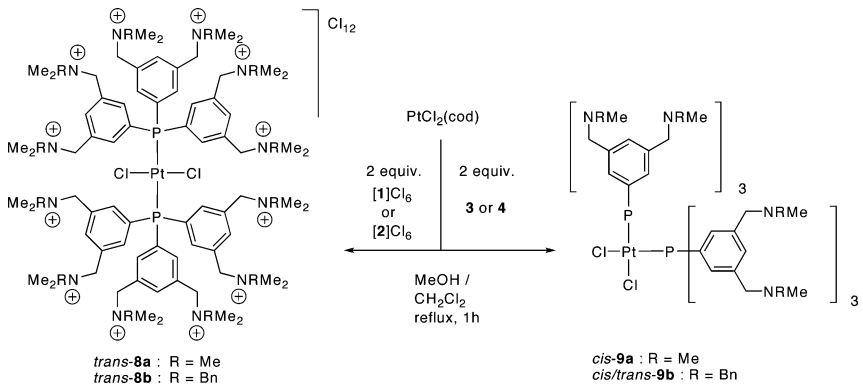

Scheme 1 The reaction of hexacationic and neutral ligands with $PtCl_2$(cod).

not return after cooling to room temperature.[13] Due to its labile nature, this species could not be identified, but the magnitude of the observed ^{31}P–^{195}Pt coupling constant rules out the possibility that it corresponds to a complex of the type *cis*-$[PtCl_2L_2]Cl_{12}$ (L = **1**, **2**).[10]

The neutral ligand **3**, which is sterically similar to [**1**]$^{6+}$ and bears six aminomethyl groups instead of ammoniomethyl groups, has previously been reported to form the complex *cis*-$PtCl_2$(**3**)$_2$ (**9a**) upon reaction with $PtCl_2$(cod) in C_6D_6 (Scheme 1).[14] The reaction of two equiv. of its larger benzylamine analogue **4**, which is sterically similar to [**2**]$^{6+}$,[9d] with $PtCl_2$(cod) gave a mixture of *cis*- and *trans*-$PtCl_2$(**4**)$_2$ (**9b**), in a ratio of 70 : 30 in DMSO-d_6 and 85 : 15 in toluene-d_8 (Table 1, entries 12, 13).[15] The analogous reaction of benchmark ligand PPh_3 exclusively yielded *cis*-$PtCl_2(PPh_3)_2$ in DMSO-d_6 (entry 15). The commercially available ligand P(4-$CF_3C_6H_4)_3$ is a significantly less strongly σ-donating ligand than PPh_3. Its σ-donating strength is comparable to those of both [**1**]$^{6+}$ and [**2**]$^{6+}$.[9d] The reaction of two equiv. of P(4-$CF_3C_6H_4)_3$ with $PtCl_2$(cod) in DMSO-d_6 yielded exclusively *cis*-$PtCl_2$(P(4-$CF_3C_6H_4)_3)_2$ (entry 16).

2.2 Investigations into the mechanism of the reaction of [1]$^{6+}$ or [2]$^{6+}$ with $PtCl_2$(cod)

In order to investigate the mechanism of formation of the complexes *trans*-$[PtCl_2L_2]^{12+}$ (L = **1**, **2**), the reaction of one and subsequently two equiv. of [**1**]$^{6+}$ or [**2**]$^{6+}$ with $PtCl_2$(cod) was studied. These reactions were carried out in an NMR tube, by mixing the reactants in DMSO-d_6 for 1 min at room temperature, followed by heating at 65° for 15–30 min. The products were not isolated but were directly characterized by ^{31}P-NMR and ESI-MS. Using one equiv. of [**1**]Cl_6 or [**2**]Cl_6, the observation of a sharp singlet by ^{31}P-NMR indicated the formation of a single species in both cases (Table 1, entries 3 and 8). ESI-MS analysis of the reaction mixtures showed fragments containing one phosphine per Pt centre, *i.e.* $[PtL]Cl_{(8-n)}^{n+}$ (L = **1**, **2**; *n* = 2, 3. Table 2, entries 3 and 4). The analogous reaction of PPh_3 yielded a mixture of *cis*- and *trans*-$PtCl_2(PPh_3)_2$, *cis*-$PtCl_2$(DMSO)(PPh_3) and unreacted $PtCl_2$(cod).[16,17] When this reaction was performed in the presence of 6 equiv. of NBu_4Cl, a fourth signal was observed, corresponding to the anion $[PtCl_3PPh_3]^-$ (Table 1, entry 14).[18] In view of the

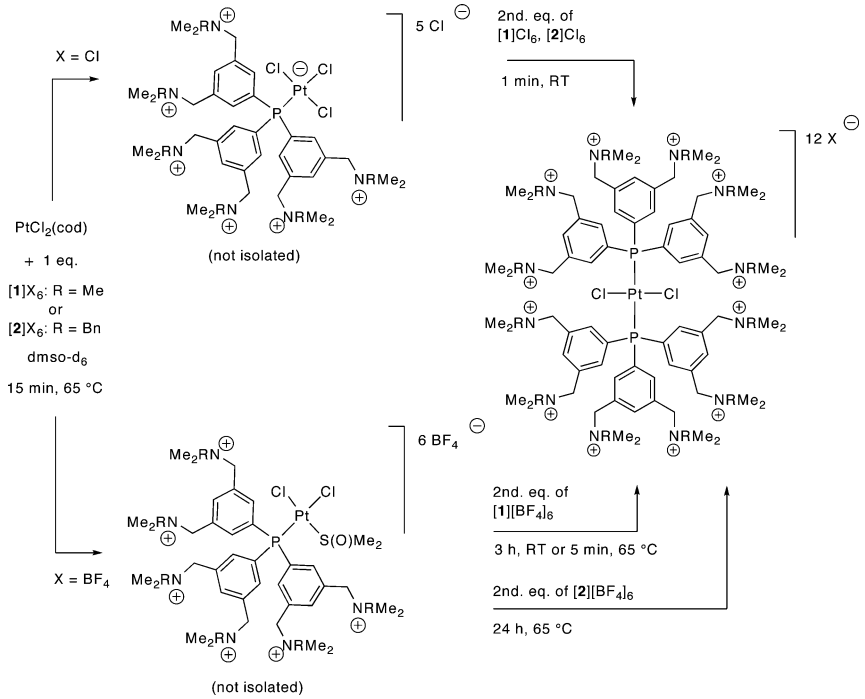

Scheme 2 Effect of the presence of free chloride on the coordination chemistry of $[\mathbf{1}]^{6+}$ and $[\mathbf{2}]^{6+}$ with Pt(II) in DMSO-d_6.

similarity of the ^{31}P-NMR spectra of the products obtained for the reactions of [**1**]Cl$_6$ and [**2**]Cl$_6$ to that of $[PtCl_3PPh_3]^-$ (Table 1, entries 3, 8 and 14), the observed products were assigned the structures [PtCl$_3$(**1**)]Cl$_5$ and [PtCl$_3$(**2**)]Cl$_5$ (Scheme 2). The ESI-MS measurements are consistent with these structures. The reaction of one equiv. of **4** with PtCl$_2$(cod) in DMSO-d_6 resulted in a mixture of *cis*- and *trans*-**9b**, a third, unidentified product (δ 19 ppm, presumably PtCl$_2$(DMSO)(**4**)) and unreacted PtCl$_2$(cod).

The analogous reaction of one equiv. of the chloride-free ligands [**1**][BF$_4$]$_6$ or [**2**][BF$_4$]$_6$ also led to the formation of one major species in both cases, but the ^{31}P-NMR spectra of the products were clearly different from those obtained with [**1**]Cl$_6$ and [**2**]Cl$_6$ (Table 1, entries 3 and 8 *vs.* entries 5 and 10). The ^{31}P-NMR data found for these species closely match those for *cis*-PtCl$_2$(DMSO)(PPh$_3$) (entry 14). Analysis by ESI-MS showed signals corresponding to the ions $[PtCl_2(DMSO)(L)][BF_4]_{(6-n)}^{n+}$ (L = **1**, **2**; n = 2, 3. Table 2, entries 5 and 6). The major products were therefore assigned the structures *cis*-[PtCl$_2$(DMSO)(L)][BF$_4$]$_6$ (L = **1**, **2**).

The ^{31}P-NMR spectrum of the solution obtained after mixing one equiv. of [**1**][BF$_4$]$_6$ with PtCl$_2$(cod), apart from the intense sharp singlet attributed to [PtCl$_2$(DMSO)(**1**)][BF$_4$]$_6$, showed a minor, broad signal at 9.1 ppm, which corresponds to the chemical shift observed for [PtCl$_3$(**1**)]Cl$_5$.[19] Therefore, we propose that [PtCl$_2$(DMSO)(**1**)][BF$_4$]$_6$ in DMSO solution exists in equilibrium with [PtCl$_3$(**1**)][BF$_4$]$_5$ and, presumably, [PtCl(DMSO)$_2$(**1**)][BF$_4$]$_7$. Added amounts of the free chloride should diminish the concentrations of [PtCl$_2$(DMSO)(**1**)]X$_6$ and [PtCl(DMSO)$_2$(**1**)][X]$_7$ in favour of [PtCl$_3$(**1**)]X$_5$ (X = Cl, BF$_4$). Indeed, when increasing amounts (0.4–2.0 equiv. with respect to Pt) of NBu$_4$Cl were added to a solution of [PtCl$_2$(DMSO)(**1**)][BF$_4$]$_6$, the signal for the latter species gradually disappeared, while that for [PtCl$_3$(**1**)]X$_5$ gained intensity. When an excess of NBu$_4$Cl was added, only the signal for [PtCl$_3$(**1**)]X$_5$ was observed.

Upon addition of a second equiv. of [**1**]Cl$_6$ or [**2**]Cl$_6$, respectively, to a solution of [PtCl$_3$L]Cl$_5$ (L = **1**, **2**), the immediate and quantitative formation of *trans*-[PtCl$_2$L$_2$]Cl$_{12}$ (L = **1**, **2**) (*i.e.* **8a**,**b**) was observed by ^{31}P-NMR. In contrast, when a second equiv. of [**1**][BF$_4$]$_6$ or [**2**][BF$_4$]$_6$, respectively, was added to a solution of [PtCl$_2$(DMSO)(L)][BF$_4$]$_6$ (L = **1**, **2**), initially no further reaction occurred and the added free ligand remained uncoordinated in solution, as observed by ^{31}P-NMR. When the solutions were stirred for a prolonged period, eventually quantitative formation of *trans*-[PtCl$_2$L$_2$][BF$_4$]$_{12}$ (L = **1**, **2**) was observed (Scheme 2). In the case of the reaction between [PtCl$_2$(DMSO)(**1**)][BF$_4$]$_6$ and [**1**][BF$_4$]$_6$, the reaction took 3 h at room temperature to go to completion. The identity of the product *trans*-[PtCl$_2$(**1**)$_2$][BF$_4$]$_{12}$ was confirmed by ^{31}P-NMR (Table 1, entry 6) and ESI-MS (Table 2, entry 7). When the reaction was performed at 65 °C, complete conversion was obtained after 5 min. The reaction of [PtCl$_2$(DMSO)(**2**)][BF$_4$]$_6$ with [**2**][BF$_4$]$_6$ was much slower: stirring at 65 °C for 24 h was required for complete conversion to the product *trans*-[PtCl$_2$(**2**)$_2$][BF$_4$]$_{12}$.

2.3 The reactions of [1]I$_6$, [5]I$_4$, [6]I$_2$ and [7]I$_3$ with PtI$_2$(cod)

The reaction of two equiv. of [**1**]I$_6$ with PtI$_2$(cod), in either refluxing MeOH–CH$_2$Cl$_2$ or in H$_2$O at room temperature, resulted in the exclusive formation of *trans*-[PtI$_2$(**1**)$_2$]I$_{12}$ (**10a**) (Scheme 3). The ^{31}P-NMR spectrum measured in D$_2$O showed one singlet at δ 16.2 ppm with Pt satellites ($^1J_{P,Pt}$ = 2583 Hz). No isomerization to the *cis* isomer was observed, not even at higher temperatures and in the presence of free hexacationic ligand. For tetra-*meta*-ammoniomethyl substituted [**5**]I$_4$, di-*meta*-ammoniomethyl substituted [**6**]I$_2$ and tri-*para*-ammoniomethyl substituted [**7**]I$_3$, the reaction with PtI$_2$(cod) in MeOH–CH$_2$Cl$_2$ yielded mixtures of *cis*- and *trans*-isomers of the complexes [PtI$_2$(**5**)$_2$]I$_8$ (**10b**), [PtI$_2$(**6**)$_2$]I$_4$

Table 3 ^{31}P-NMR data for the products of the respective reactions of [**1**]I_6, [**5**]I_4, [**6**]I_2 and [**7**]I_3 with PtI_2(cod)

					^{31}P-NMR		
Entry	L	L/Pt	Solvent	Product(s)	δ (ppm)	$^1J_{P,Pt}$ (Hz)	% obs.
1	[**1**]I_6	2	D_2O	*trans*-[PtI_2(**1**)$_2$]I_{12} (**10a**)	16.4	2583	100
2	[**1**]I_6	2	DMSO-d_6	*trans*-[PtI_2(**1**)$_2$]I_{12} (**10a**)	13.8	2520	80
				[PtI_3(**1**)]I_5	11.4	3596	20
				[**1**]I_6	–3.3		
3	[**1**]I_6	1	DMSO-d_6	[PtI_3(**1**)]I_5	11.4	3596	100
4	[**5**]I_4	2	D_2O	*trans*-[PtI_2(**5**)$_2$]I_8 (**10b**)	12.7	2498	100
5	[**5**]I_4	2	DMSO-d_6	*trans*-[PtI_2(**5**)$_2$]I_8 (**10b**)	11.6	2488	90
6[a]	[**6**]I_2	2	D_2O	*trans*-[PtI_2(**6**)$_2$]I_4 (**10c**)	12.6	2478	25
				cis-[PtI_2(**6**)$_2$]I_4 (**10c**)	13.2	3479	75
7	[**6**]I_2	2	DMSO-d_6	*trans*-[PtI_2(**6**)$_2$]I_4 (**10c**)	12.4	2478	80
				cis-[PtI_2(**6**)$_2$]I_4 (**10c**)	11.8	3471	20
8	[**7**]I_3	2	D_2O	*trans*-[PtI_2(**7**)$_2$]I_6 (**11**)	12.0	2467	55
				cis-[PtI_2(**7**)$_2$]I_6 (**11**)	11.3	3491	45
9	PPh_3	2	$CDCl_3$	*trans*-$PtI_2(PPh_3)_2$	13.1	2491	80
				cis-$PtI_2(PPh_3)_2$	12.4	3455	20

[a] Measured at 45 °C.

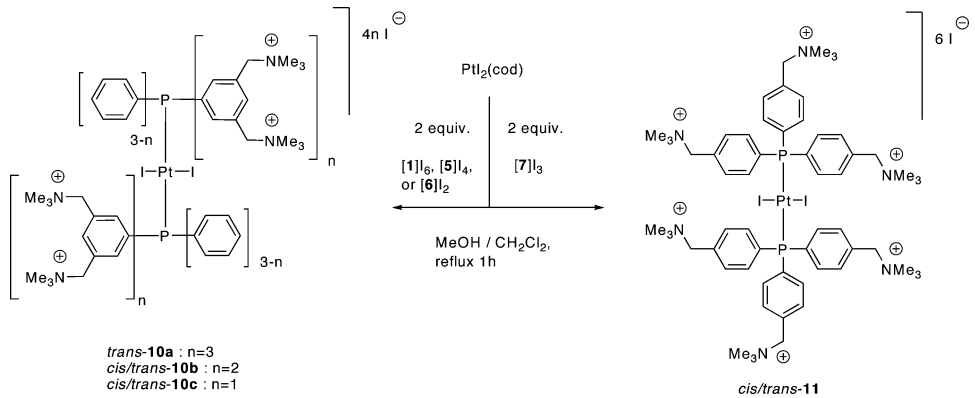

Scheme 3 The reactions of di- tri- tetra- and hexacationic ligands with PtI_2(cod).

(**10c**) and [PtI_2(**7**)$_2$]I_6 (**11**) (Scheme 3), as indicated by their ^{31}P-NMR spectra, measured in either D_2O or DMSO-d_6 (Table 3). In the ^{13}C-NMR spectra of **10a–c** and **11**, the *ipso*- and *ortho*-carbons of the aryl rings were observed as *pseudo* triplets, indicating the presence of an AA′X system (A = ^{31}P, X = ^{13}C),[20] which is consistent with the coordination of two phosphine ligands to the Pt centre. In the case of **10b**, only the *trans*-isomer was observed in D_2O, while a small amount of the *cis*-isomer was observed in DMSO-d_6 (10%). For **10c**, the *cis*-isomer was favoured in D_2O (75 : 25), while in DMSO-d_6 the *trans*-isomer was favoured (20 : 80).[21] *Trans*-**10b** and *trans*-**10c** have very similar chemical shifts and $^1J_{P,Pt}$ coupling constants in ^{31}P-NMR (with a difference of 0.1 ppm and 20 Hz, respectively, in D_2O), while *trans*-**10a** has a chemical shift that is 3.7 ppm higher and a $^1J_{P,Pt}$ coupling constant that is 85 Hz higher than that of *trans*-**10b** (Table 3). The origin of this difference is unclear.

For [PtI_2(**7**)$_2$]I_6 (**11**), a small excess of the *trans* isomer was present in D_2O at room temperature (55 : 45). Complex **11** readily isomerized upon increasing the temperature,[22] leading to a shift of the equilibrium to the side of the *trans* isomer. Upon cooling down, the original distribution was restored. Furthermore, the position of this equilibrium was found to be dependent on the ionic strength of the solution (Fig. 3). The addition of NaI up to a concentration of 0.2 M led to a shift to the side of the *cis*-isomer. Increasing

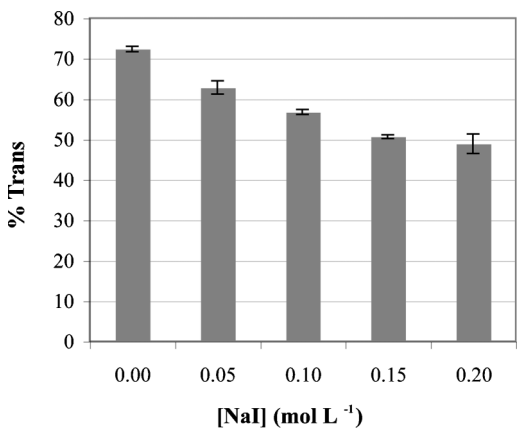

Fig. 3 The dependence of the *trans*/*cis* equilibrium position of [PtI_2(**7**)$_2$]I_6 (**11**) on the concentration of added NaI, at 65 °C.

the temperature, both in the absence and in the presence of 0.2 M NaI, allowed the calculation of the thermodynamic parameters (Table 4) for *trans*- to *cis*-isomerization in both cases, using Van 't Hoff plots (Fig. 4). These values show that *trans*- to *cis*-conversion results in a significantly larger negative enthalpy change in the presence of 0.2 M NaI, confirming the stabilization of the *cis*-isomer by the added NaI.

Table 4 Enthalpy and entropy changes for *trans*- to *cis*-isomerization of $[PtI_2(7)_2]I_6$ (**11**)

[NaI] (mol L^{-1})	ΔH (kJ mol^{-1})	ΔS (J mol^{-1} K^{-1})
0.0	–22.0	–73.1
0.2	–32.3	–95.0

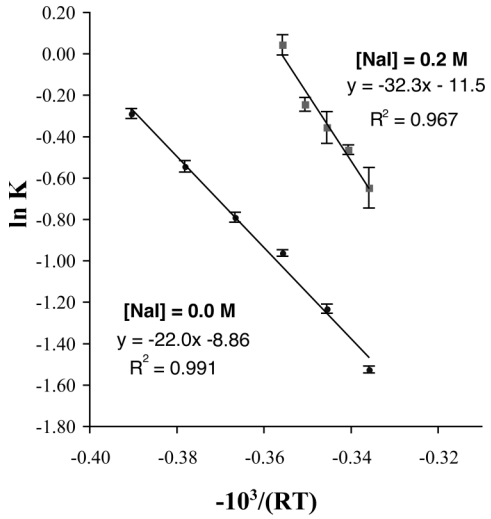

Fig. 4 Van 't Hoff plots for *trans*- to *cis*-isomerization of $[PtI_2(7)_2]I_6$ (**11**), at 0.0 M NaI (25–85 °C) and at 0.2 M NaI (65–85 °C).

2.4 Structure and reactivity of *trans*-$[PtI_2(1)_2]I_{12}$ (10a)

Crystals of *trans*-$[PtI_2(\mathbf{1})_2]I_{12}$ (**10a**), suitable for single-crystal X-ray structure determination, were grown from a concentrated solution of **10a** in hot H_2O, which was allowed to cool down to room temperature. The molecular structure of *trans*-**10a** is depicted in Fig. 5 and selected bond lengths and angles are given in Table 5. In the cation of *trans*-**10a**, the Pt(II) centre, which is found at a site of inversion symmetry, is bonded to two iodide ligands and two phosphine ligands in a *trans* square planar geometry. The

Table 5 Selected bond lengths and angles of *trans*-$[PtI_2(\mathbf{1})_2]I_{12}$ (**10a**)

Bond length (Å)		Angle (°)		Angle (°)
Pt1-P1	2.3163 (10)	I1-Pt1-P1	91.15(3)	C11-P1-C21 107.41(18)
Pt1-I1	2.6136(3)	P1-Pt1-I1a	88.84(3)	C11-P1-C31 98.86(19)
P1-C11	1.831(4)	Pt1-P1-C11	115.46(14)	C21-P1-C31 103.44(18)
P1-C21	1.828(4)	Pt1-P1-C21	112.07(13)	
P1-C31	1.833(4)	Pt1-P1-C31	118.06(13)	

inclination angles found between the planes of the three aryl rings with respect to the P–Pt axis of direction are 5.88(17)°, 9.60(17)° and 63.22(16)° and show a significant deviation from a C_3-symmetrical propeller-shape. Thus, the P–Pt axis of direction is roughly parallel to the mean molecular planes of two of the three independent aryl rings. Two of the six free iodide anions per phosphine ligand (I2 and I3, Fig. 5) are embedded in cationic pockets formed by several of the ammonium groups, while the other anions (*i.e.* I4–I8) are located in between adjacent molecules in the crystal lattice. Iodides I6 (I6A/I6B) and I8 (I8A/I8B) are disordered and are split over two positions. Iodides I7 and I8A/B both have a population occupancy of 0.5 (further details about the refinement can be found in the experimental section). Finally, based on the crystal structure of *trans*-**10a**, a Tolman cone angle[31] of 195° can be estimated for $[\mathbf{1}]I_6$ using the method of Müller and Mingos.[23] However, this value seems to be overestimated (see Discussion).

Trans-$[PtI_2(\mathbf{1})_2]I_{12}$ (**10a**) is stable up to a temperature of 85 °C in D_2O. In contrast, upon dissolving *trans*-**10a** in DMSO-d_6, a ligand exchange of $[\mathbf{1}]I_6$ for iodide occurred, forming $[PtI_3(\mathbf{1})]I_5$ (δ = 11.4 ppm, $^1J_{P,Pt}$ = 3596 Hz, Scheme 4) and uncoordinated $[\mathbf{1}]I_6$. Such reactivity was not observed for complexes **10b** and **10c**, not even at high temperatures. When PtI_2(cod) was reacted with 1 equiv. of $[\mathbf{1}]I_6$ in DMSO-d_6, $[PtI_3(\mathbf{1})]I_5$ was formed quantitatively. An ESI-MS spectrum of this solution showed the fragments $[Pt(\mathbf{1})I_{(8-n)}]^{n+}$ (n = 2, 3, 4) (Table 2, entry 8). Upon increasing the temperature, the ratio $[PtI_3(\mathbf{1})]I_5$ + $[\mathbf{1}]I_6$: *trans*-$[PtI_2(\mathbf{1})_2]I_{12}$ increased from 0.25 at room temperature, to 1.0 at 85 °C. After cooling down, the initial product distribution was restored. Addition of one equiv. of molecular iodine to a solution of **10a**

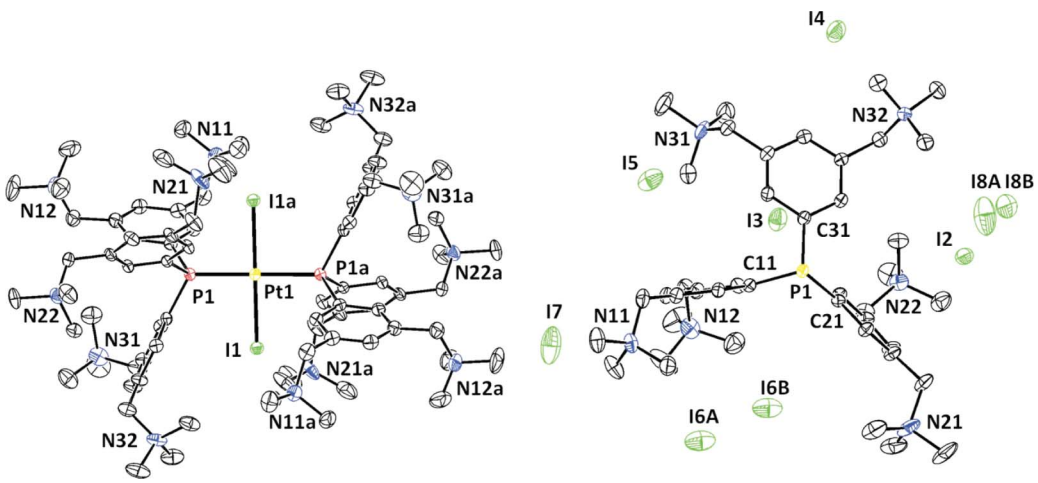

Fig. 5 Displacement ellipsoid plots (50% probability level) of *trans*-$[PtI_2(\mathbf{1})_2]I_{12}$ (**10a**) given at 150(2) K. Left: hydrogen atoms and lattice iodide counter anions have been omitted for clarity. One half of the molecule is generated by inversion symmetry. Right: the crystallographically independent phosphine ligand and lattice iodide counter anions viewed down the direction of the P–Pt–P axis. Hydrogen atoms have been omitted for clarity.

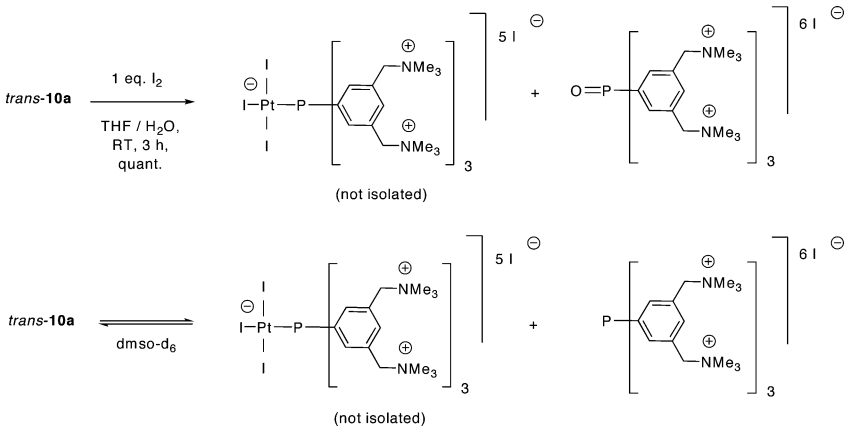

Scheme 4 The two ways of formation of $[PtI_3\mathbf{1}]I_5$ from *trans*-**10a**.

in THF–H_2O also led to the formation of $[PtI_3(\mathbf{1})]I_5$ (δ 13.8 ppm, $^1J_{P,Pt}$ = 3620 Hz, D_2O) (Scheme 4).[24] In this reaction, one equiv. of the phosphine oxide of $[\mathbf{1}]I_6$ was formed as a coproduct and identical reactivity was observed for **10b** and **10c**. No Pt(IV) species were observed by ^{31}P-NMR. When I_2 was added to a solution of $PtI_2(PPh_3)_2$ in $CHCl_3$–THF, no reaction occurred, but when the reaction was carried out in the presence of NBu_4I and H_2O, a reactivity similar to that of **10a–c** was observed, forming $[NBu_4][PtI_3PPh_3]$ (δ 12.1 ppm, $^1J_{P,Pt}$ = 3631 Hz, $CDCl_3$).[25]

Crystals were grown from a concentrated solution of $[PtI_3(\mathbf{1})]I_5$ in D_2O. The molecular structure of $[PtI_3(\mathbf{1})]I_5$ is depicted in Fig. 6 and selected bond lengths and angles are given in Table 6. The crystal structure shows that the Pt(II) ion is bonded to one phosphine ligand and three iodide ligands and is found in a distorted square planar geometry. The Pt centre bears a formal negative charge, leaving five remaining lattice counterions, found near the hexacationic phosphine ligand, for charge balance. The sum of occupancy factors for all lattice iodides (*i.e.* I4-I9) is 5 (further details about the refinement can be found in the experimental section). Two of these iodides (I6 and I8) are embedded in cationic pockets formed by the ammonium groups.

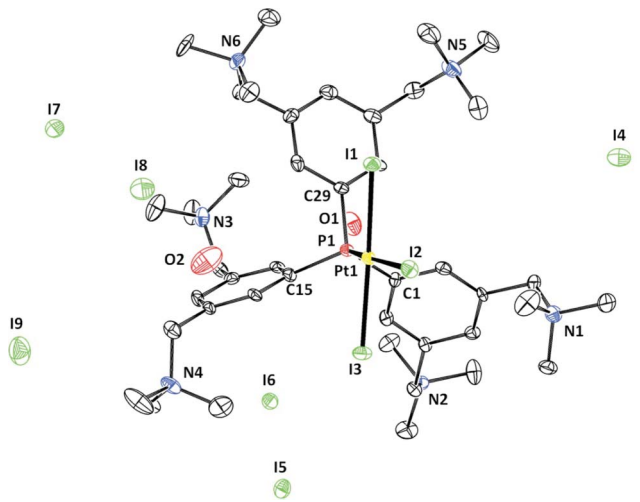

Fig. 6 Displacement ellipsoid plot (50% probability level) of $[PtI_3(1)]I_5$ given at 110(2) K. Hydrogen atoms have been omitted for clarity.

Table 6 Selected bond lengths and angles of $[PtI_3(\mathbf{1})]I_5$

	Bond length (Å)		Angle (°)		Angle (°)
Pt1-P1	2.2196 (18)	I1-Pt1-I2	88.620(17)	Pt1-P1-C1	105.7 (2)
Pt1-I1	2.5824(5)	I1-Pt1-I3	176.95(2)	Pt1-P1-C15	120.7(3)
Pt1-I2	2.6460(5)	I1-Pt1-P1	92.83(5)	Pt1-P1-C29	117.6(2)
Pt1-I3	2.6207(7)	I2-Pt1-I3	89.822(17)	C1-P1-C15	106.8(3)
P1-C1	1.811(7)	I2-Pt1-P1	170.23(5)	C1-P1-C29	106.2(3)
P1-C15	1.807(7)	I3-Pt1-P1	89.15(5)	C15-P1-C29	98.3(3)
P1-C29	1.830(7)				

Table 7 Selected bond lengths and angles in the crystal structures of complexes of the type *trans*-PtI_2L_2 (L = monodentate phosphine) and the Tolman cone angles of the corresponding phosphines

P-Ligand	CPC (°)	P–Pt (Å)	P–C (Å)	Ref.	Cone Angle (°)
PPh_3	107.6(3) 103.2(3) 101.7(3)	2.318(2)	1.826(4)	26a	145[a]
$P(Cy)_3$	104.96 108.33 102.19	2.371(2)	1.844(8) 1.861(10) 1.891(9)	26c	170[a]
$[\mathbf{1}]^{6+}$	107.41(18) 98.86(19) 103.44(18)	2.3165(10)	1.830(4)	this work	195[b], 150[c]

[a] Tolman cone angle, determined from CPK molecular models, see ref. 31 [b] Estimated from the X-ray crystal structure of *trans*-$[PtI_2(\mathbf{1})_2]I_{12}$ (**10a**). [c] Estimated from the ^{31}P-NMR chemical shift of the complex $[PdCl_2(\mathbf{1})_2]Cl_{12}$.

3 Discussion

3.1 Crystal structures of *trans*-$[PtI_2(1)_2]I_{12}$ (10a) and $[PtI_3(1)]I_5$.

In complexes of the type *trans*-PtI_2L_2 (L = monodentate phosphine ligand), the Pt–P bond length, as well as the C–P–C angles and the C–P bond lengths in the phosphine, are known to increase with an increasing steric demand of the phosphine ligand.[26] For *trans*-$[PtI_2(\mathbf{1})_2]I_{12}$ (**10a**), these geometrical parameters are very similar to those found in *trans*-$PtI_2(PPh_3)_2$ (Table 7), indicating that no significant increase in the steric congestion is present in *trans*-**10a**.

In the structure of $[PtI_3(\mathbf{1})]I_5$, the bond length between the Pt centre and the I atom *trans* to the phosphine is about 0.016 Å shorter than in $[NBu_4][PtI_3(PPh_3)]$.[25] This suggests a weaker *trans*-influence of $[\mathbf{1}]^{6+}$ compared to PPh_3. This is consistent with the

weaker σ-donating strength of $[\mathbf{1}]^{6+}$, which we have previously demonstrated by evaluation of the $^{1}J_{P,Se}$ coupling constants in ^{31}P-NMR of the corresponding phosphine selenides.[9d]

Even though the geometrical parameters for *trans*-**10a** given in Table 7 do not indicate an increased steric congestion compared to *trans*-$PtI_2(PPh_3)_2$, the bulky character of $[\mathbf{1}]^{6+}$ as a ligand is evident from the overall shape of the phosphine in the structure of *trans*-**10a** (Fig. 5). Based on this structure, a cone angle of 195° can be estimated for $[\mathbf{1}]^{6+}$.[23] The structures of *trans*-**10a**, $[PtI_3(\mathbf{1})]I_5$ and previously reported $[\mathbf{1}(S)]I_6$[9d] show clear differences in the positioning of the cations and anions, as well as in the conformations of the aryl rings and ammoniomethyl substituents. This indicates that these structures are relatively flexible and adopt different conformations upon crystallizing, which leads to significant differences in the cone angles obtained from each of the three structures. In all cases, the sterically demanding conformation in the solid state, *i.e.* the coplanarity of the aryl rings with respect to the P–Pt axis of direction, is adopted in order to accommodate the large iodide ions in the cationic pockets. In polar solvents, this conformation is probably not retained due to solvent separated ion pairing,[27] leading to an overall smaller effective cone angle in solution. Indeed, when the cone angles of $[\mathbf{1}]^{6+}$ and $[\mathbf{2}]^{6+}$, respectively, were estimated by measuring the ^{31}P-NMR chemical shifts of the complexes *trans*-$[PdCl_2L_2]Cl_{12}$ (L = **1**, **2**),[9d] a much smaller value of approximately 150° was found in both cases, which seems to be in better agreement with the geometrical parameters in Table 7. These NMR spectra were measured in CD_3OD, ensuring minimal ion pairing and the value can thus be attributed to the cone angle of the 'naked' cations $[\mathbf{1}]^{6+}$ and $[\mathbf{2}]^{6+}$.

3.2 Effects of Coulombic inter-ligand repulsion forces

Differences in the thermodynamic stabilities of *cis*- and *trans*-isomers of species of the type PtX_2L_2 (L = tertiary phosphine, X = halide) have been described in detail in the literature and are ascribed to a complex combination of factors.[28,29] The differences in bond energies between the *cis*- and *trans*-isomers originate mainly from the differences in the respective *trans*-influences of the tertiary phosphine ligand L and the halide ligand X and favour the *cis*-isomers.[30] Coulombic interactions between the partial negative charges on X and the partial positive charges on Pt and L favour the *trans*-isomers. Due to the large difference in the dipole moments of the isomers, the solvation effects favour the *cis*-isomers in polar solvents and the *trans*-isomers in apolar solvents. Finally, when bulky phosphine ligands are used, the steric repulsion favours the *trans*-isomers.[31,32] Each of these factors has its own effect on the thermodynamic stability of the respective isomers and these are often finely balanced. The *cis*-*trans* isomerization of these complexes is in most cases catalyzed by free phosphine, free halide or a solvent molecule.[29]

The complete selectivity of the hexacationic ligands $[\mathbf{1}]^{6+}$ and $[\mathbf{2}]^{6+}$ towards the formation of the *trans*-isomers of the complexes $[PtCl_2L_2]Cl_{12}$ (L = **1**, **2**), without subsequent *trans*- to *cis*-isomerization, indicates that a large energetic difference exists between the *trans*- and *cis*-isomers of these complexes. In contrast, the neutral ligands **3** and **4** form the corresponding *cis*-isomers either exclusively or predominantly. For $PtCl_2(\mathbf{4})_2$ (**9b**), *cis*- to *trans*-isomerization was observed upon heating in the presence of free **4**, indicating that the *cis*-isomer is thermodynamically favoured. ^{31}P-NMR chemical shifts of the corresponding complexes *trans*-$PdCl_2L_2$ (L = $[\mathbf{2}]^{6+}$, **4**),[9d] have earlier pointed out that the neutral ligand **4** is sterically similar to $[\mathbf{2}]^{6+}$. This observation suggests that steric factors do not play an important role in the behaviour of $[\mathbf{1}]^{6+}$ and $[\mathbf{2}]^{6+}$. The electron donating ability of a phosphine ligand may, through its *trans*-influence, also influence the preference for the *cis*- or *trans*-isomers. By measuring the coupling constant $^{1}J_{P,Se}$ in the ^{31}P-NMR spectrum of the corresponding phosphine selenides, we have previously established that the σ-donating ability of both $[\mathbf{1}]^{6+}$ and $[\mathbf{2}]^{6+}$ is significantly less strong than that of PPh_3 and is comparable to that of $P(4\text{-}CF_3C_6H_4)_3$.[9d] The latter ligand forms the complex *cis*-$PtCl_2(P(4\text{-}CF_3C_6H_4)_3)_2$ exclusively, indicating that the reduced σ-donating strength, and thus the weaker *trans*-influence of these phosphines, probably does not play an important role either in their preference for the formation of *trans*-complexes. Importantly, the ^{31}P-NMR measurements for each of these complexes (see Table 1) were performed in the same solvent, *i.e.* DMSO-d_6, thus eliminating the influence of the solvent in these comparisons. Instead, repulsive Coulombic forces between the coordinated ligands in complexes of the type $PtCl_2L_2$ (L = $[\mathbf{1}]^{6+}$, $[\mathbf{2}]^{6+}$) seem to be the dominating factor in their exclusive formation of the *trans*-isomers. Such repulsive forces are stronger in the *cis*-complexes due to the closer proximity of the ligands, explaining the higher thermodynamic stability of the *trans*-isomers.

More evidence for the importance of the Coulombic inter-ligand repulsion forces in this type of complex is provided by the observation that the *cis*-*trans*-equilibrium position of $[PtI_2(\mathbf{7})_2]I_6$ (**11**) is dependent on the ionic strength of the solution. Increasing the NaI concentration leads to a shift in the equilibrium to the side of the *cis*-isomer. Therefore, we propose that the repulsive Coulombic interaction, which disfavours the *cis*-isomer, is attenuated at higher ionic strengths due to the shielding of the charges. Furthermore, the increased polarity of the medium upon increasing the ionic strength[33] may favour the *cis*-isomer due to its large dipole moment. No further shift was observed at concentrations higher than 0.15 M. It is likely that at this concentration, other factors begin to dominate, such as steric factors as well as the respective *trans*-influences of the ligands. Several examples are found in the literature where related repulsive Coulombic interactions have been put forward as the driving force for the formation of square planar *trans*-complexes; yet, in none of these cases has this explanation been substantiated. Hexa-anionic tris-*para*-phosphonated triphenylphosphine (*p*-TPPTP) forms the *trans*-isomer of the complex $PtCl_2(p\text{-TPPTP})_2$ exclusively (in D_2O).[34] The palladium(II) complex *cis*-$PdCl_2[P(CH_2)_2NMe_2)_3]_2$ was shown to undergo quantitative *cis*- to *trans*-isomerization upon protonation of the dimethylamino groups.[35] Yet, trianionic tris-*meta*-sulfonated triphenylphosphine (TPPTS) forms predominantly the *cis*-isomer of the complex $PtCl_2(TPPTS)_2$ (*cis* : *trans* = 80 : 20 at RT in DMSO-d_6).[36] It is likely that similar repulsive Coulombic forces exist in this complex, although in this case they apparently do not outweigh the contributions of other factors.

As mentioned above, the repulsive Coulombic forces between the ligands coordinated to Pt(II) have for a long time been known to contribute to the total of factors governing *cis*-*trans*-equilibria and can be rationalized by a release of inter-ligand repulsive forces in the *trans*-isomers with respect to the *cis*-isomers. This effect has previously been described to originate from the *partial* negative charges on the halide ligands and the *partial* positive charges

on the phosphine ligands.[28] The phosphine ligands considered in the present study carry permanent *ionic* groups. Based upon our own observations as well as those of others,[34,35] we believe that the commonly accepted principle of repulsive Coulombic inter-ligand interaction can be invoked to describe the behaviour of these oligocationic phosphine ligands.

Trans-$[PtI_2(\mathbf{1})_2]I_{12}$ (**10a**) partially dissociates in DMSO-d_6 solution, establishing an equilibrium with $[PtI_3\mathbf{1}]I_5$ and uncoordinated $[\mathbf{1}]I_6$. In contrast, such dynamic behaviour was not observed for $[PtI_2(\mathbf{5})_2]I_8$ (**10b**), $[PtI_2(\mathbf{6})_2]I_4$ (**10c**) or *trans*-$[PtCl_2(\mathbf{1})_2]Cl_{12}$ (**8a**), not even at elevated temperatures. This suggests that the increase in steric and Coulombic repulsion forces going from **10c** and **10b** to **10a** destabilizes the complex. In the crystal structure of *trans*-**10a**, values found for the Pt–P and C–P bond lengths and the C–P–C angles are very similar to those found in *trans*-$PtI_2(PPh_3)_2$ (*vide supra*).[26a] As these parameters are known to be sensitive to the steric bulk of the phosphine, this indicates that the steric demand of $[\mathbf{1}]I_6$ is most likely not the main reason for the observed lability of *trans*-**10a** and suggests an important role for the repulsive Coulombic forces. The difference in stability upon dissolution in DMSO-d_6, between *trans*-$[PtCl_2(\mathbf{1})_2]Cl_{12}$ (**8a**) and *trans*-$[PtI_2(\mathbf{1})_2]I_{12}$ (**10a**) indicates that the anion plays an important role as well and could originate from a higher thermodynamic stability of the product $[PtX_3(\mathbf{1})]X_5$ for X = I compared to X = Cl. Thus, the nature of the phosphine ligand, the anion and the solvent each contribute to the dynamic behaviour observed for **10a**.

3.3 Mechanism of formation of *trans*-$[PtCl_2L_2]^{12+}$ (L = 1, 2).

In the reaction of one equiv. of the phosphines $[\mathbf{1}]Cl_6$ or $[\mathbf{2}]Cl_6$ with $PtCl_2$(cod) in DMSO-d_6, a complete selectivity towards the formation of the complexes $[PtCl_3L]Cl_5$ (L = **1**, **2**) was observed. In contrast, the analogous reaction of neutral **4** and that of PPh_3, even when carried out in the presence of NBu_4Cl (6 equiv. with respect to PPh_3) yielded a mixture of products, including a significant amount of *cis*-$PtCl_2L_2$ (L = **4**, PPh_3). This suggests that the reaction of the free phosphines $[\mathbf{1}]Cl_6$ or $[\mathbf{2}]Cl_6$ with $PtCl_2$(cod) proceeds much faster than the subsequent reaction with $[PtCl_3L]Cl_5$ (L = **1**, **2**) to form *trans*-$[PtCl_2L_2]Cl_{12}$ (**8a**,**b**). Based on our considerations outlined above, we attribute this observation to repulsive Coulombic interactions between the free cationic phosphines $[\mathbf{1}]^{6+}$ or $[\mathbf{2}]^{6+}$ and the corresponding cationic monophosphine complexes $[PtCl_3L]^{5+}$ (L = **1**, **2**). The complexes $[PtCl_3L]Cl_5$ (L = **1**, **2**) can thus be regarded as intermediates in the reaction of $[\mathbf{1}]Cl_6$ and $[\mathbf{2}]Cl_6$, respectively, with $PtCl_2$(cod) to form *trans*-**8a–b**.

The reaction of $[\mathbf{1}][BF_4]_6$ with *cis*-$[PtCl_2(DMSO)(\mathbf{1})][BF_4]_6$ required stirring for 3 h at RT to go to completion, while the reaction of $[\mathbf{1}]Cl_6$ with $[PtCl_3(\mathbf{1})]Cl_5$ was complete within 1 min (Scheme 2). The attack of $[\mathbf{1}]^{6+}$ on $[PtCl_2(DMSO)(\mathbf{1})]^{6+}$ to give *trans*-$[PtCl_2(\mathbf{1})_2]^{12+}$ thus appears to be kinetically inhibited. Substitutions at Pt(II) occur with retention of the stereochemistry.[29,37] Formation of *trans*-$[PtCl_2(\mathbf{1})_2]^{12+}$ starting from $[PtCl_3(\mathbf{1})]^{5+}$ can thus occur in one step, *i.e.* by substitution of the chloride *trans* to the phosphine in $[PtCl_3(\mathbf{1})]^{5+}$, which is favoured by the high *trans*-effect[37] of the coordinated phosphine ligand. In contrast, in $[PtCl_2(DMSO)(\mathbf{1})]^{6+}$, the phosphine and the DMSO ligands have a *cis*-configuration with respect to each other[38] and the substitution of the DMSO ligand by the incoming phosphine to form *trans*-$[PtCl_2(\mathbf{1})_2]^{12+}$ thus has to occur in two steps. Assuming that a pathway *via* the hypothetical *cis*-$[PtCl_2(\mathbf{1})_2]^{12+}$ is energetically unfavourable due to the *cis*-configuration of the two hexacationic phosphine ligands, it is plausible that the actual substitution step occurs after disproportionation of $[PtCl_2(DMSO)(\mathbf{1})]^{6+}$ into $[PtCl(DMSO)_2(\mathbf{1})]^{7+}$ and $[PtCl_3(\mathbf{1})]^{5+}$ (Scheme 5). The latter species may react with $[\mathbf{1}]^{6+}$, leading to *trans*-$[PtCl_2(\mathbf{1})_2]^{12+}$. The occurrence of such disproportionation in DMSO solution is indicated by the ^{31}P-NMR spectrum of $[PtCl_2(DMSO)(\mathbf{1})]^{6+}$, in which a minor signal attributed to $[PtCl_3(\mathbf{1})]^{5+}$ is observed.

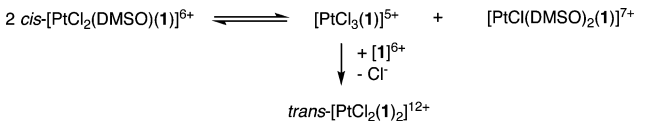

Scheme 5 Proposed mechanism of formation of *trans*-$[PtCl_2(\mathbf{1})_2]^{12+}$.

4 Conclusions

Upon combination with a Pt(II) salt, the hexacationic *meta*-ammoniomethyl-substituted ligands $[\mathbf{1}]^{6+}$ and $[\mathbf{2}]^{6+}$ lead to the exclusive formation of monophosphine-Pt(II) or *trans*-bisphosphine Pt(II) complexes. This behaviour is not matched by either neutral *meta*-aminomethyl-substituted analogues of these ligands or by triphenylphosphine and is attributed to repulsive Coulombic inter-ligand interactions. Such interactions have been put forward as the driving force for this type of coordination behaviour in some earlier cases of ionic phosphine ligands; yet, this is the first time that this explanation has been substantiated. These insights are in line with our previous studies, in which we attributed the high activity of the catalytic systems employing this class of ligands in the Pd-catalyzed Suzuki-Miyaura reaction[9b–d] to their Coulombic repulsive inter-ligand interactions.

5 Experimental

General remarks

Experiments involving free phosphines were performed using deoxygenated solvents and under an inert N_2 atmosphere using standard Schlenk techniques. Amberlite IRA-900 was purchased from Acros Chimica. $PtCl_2$(cod),[39] PtI_2(cod),[40] $[\mathbf{1}]I_6$,[9a] $[\mathbf{2}]Br_6$,[9a] $[\mathbf{5}]I_4$,[9d] $[\mathbf{6}]I_2$,[9d] $[\mathbf{7}]I_3$,[9d] $[\mathbf{1}][BF_4]_6$[9e] and $[\mathbf{2}][BF_4]_6$[9e] were synthesized according to reported literature procedures. NMR spectra were recorded on a Varian Inova 300 or a Varian AS 400 spectrometer at 25 °C unless stated otherwise. ^{1}H and ^{13}C {^{1}H} spectra were referenced to residual solvent signals. MALDI-TOF MS spectra were recorded with an Applied Biosystems Voyager System mass spectrometer using 9-nitroanthracene as the matrix. Elemental analyses were carried out by Dornis & Kolbe, Mikroanalytisches Laboratorium, Müllheim a/d Ruhr, Germany. Time-of-flight electrospray ionization mass spectra (ESI-MS) were measured by the Biomolecular Mass Spectrometry and Proteomics Group, Utrecht University, on a Micromass LC-T mass spectrometer (Waters, Manchester, UK), operating in positive ion mode. The samples were introduced at concentrations of 20–50 μM. The nanospray needle potential was typically set to 1300 V and the

cone voltage to 20–60 V. The source block temperature was set to 80 °C.

Synthesis of [1]Cl_6 and [2]Cl_6.

Hexacationic phosphines [**1**]I_6 and [**2**]Br_6 were subjected to anion exchange using an Amberlite IRA-900 (Cl) resin. Before use, the resin (70 mL, wet) was rinsed with a solution of LiCl in MeOH (0.3 M, 250 mL), until the eluate was colourless, followed by H_2O (200 mL) and MeOH (100 mL). The ion exchange was performed under a N_2 atmosphere using MeOH as the eluent (200 mL), followed by the evaporation of the solvent *in vacuo*. A column with dimensions 20–25 cm (length) and 2 cm (width) was used.

[1]Cl_6

Starting from 0.540 g of [**1**]I_6, the product was obtained as an off-white powder. Yield: 0.347 g (quant.). ^{1}H-NMR (400 MHz, CD_3OD): δ (ppm) = 8.13 (d, $^3J_{P,H}$ = 7.2 Hz, 6H, *o*-Ar), 7.89 (s, 3H, *p*-Ar), 4.71 (s, 12H, NCH_2), 3.21 (s, 54H, $N(CH_3)_3$). $^{13}C\{^1H\}$-NMR (100 MHz, CD_3OD): δ (ppm) = 141.8 (d, $^2J_{P,C}$ = 20.7 Hz, *o*-Ar), 141.5 (d, $^1J_{P,C}$ = 15.3 Hz, *i*-Ar), 139.7 (s, *p*-Ar), 131.3 (d, $^3J_{P,C}$ = 7.0 Hz, *m*-Ar), 68.8 (s, NCH_2), 53.4 (s, $N(CH_3)_3$). $^{31}P\{^1H\}$-NMR (162 MHz, CD_3OD): δ (ppm) = –2.9. HR-ESI MS: (*m*/*z*) 417.230 {$[M\text{-}2Cl]^{2+}$, calc. 417.227}.

[2]Cl_6

Starting from 0.500 g of [**2**]Br_6, the product was obtained as an off-white powder. Yield: 0.405 g (quant.). ^{1}H-NMR (300 MHz, CD_3OD): δ (ppm) = 8.30 (d, $^3J_{P,H}$ = 7.2 Hz, 6H, *o*-Ar), 7.84 (s, 3H, *p*-Ar), 7.62 (d, $^3J_{H,H}$ = 6.6 Hz, 12H, *o*-Ph), 7.53 (m, 18H, *m*- and *p*-Ph), 4.73 (s, 12H, Ph-CH_2N), 4.70 (s, 12H, Bn-NCH_2), 3.04 (s, 36H, $N(CH_3)_2$). $^{13}C\{^1H\}$-NMR (100 MHz, CD_3OD): δ (ppm) = 142.2 (d, $^2J_{P,C}$ = 19.9 Hz, *o*-Ar), 141.7 (d, $^1J_{P,C}$ = 15.0 Hz, *i*-Ar), 140.0 (s, *p*-Ar), 134.6 (s, Ph), 131.9 (s, Ph), 131.0 (d, $^3J_{P,C}$ = 7.0 Hz, *m*-Ar), 130.2 (s, Ph), 129.0 (s, Ph), 68.7 (s, NCH_2), 68.5 (s, NCH_2), 49.5 (s, $N(CH_3)_2$). $^{31}P\{^1H\}$-NMR (121 MHz, CD_3OD): δ (ppm) = –2.4. ESI MS: (*m*/*z*) 645.31 {$[M\text{-}2Cl]^{2+}$, calc. 645.32}, 418.53 {$[M\text{-}3Cl]^{3+}$, calc. 418.56}. Elem. anal. found: C 68.58, H 7.35, Cl 15.53, N 6.08, P 2.31%. Calc. for $C_{78}H_{99}Cl_6N_6P$ (1364.37): C 68.67, H 7.31, Cl 15.59, N 6.16, P 2.27%.

Synthesis of $PtCl_2L_2$ complexes 8a–b

A solution of $PtCl_2$(cod) in CH_2Cl_2 (2 mL) was added to a solution of [**1**]Cl_6 or [**2**]Cl_6 (2.0 equiv.) in MeOH (10 mL). The mixtures were heated at reflux temperature for 1 h and subsequently dried *in vacuo*.

[$PtCl_2$(**1**)$_2$]Cl_{12} (8a)

Starting from $PtCl_2$(cod) (8.5 mg, 0.023 mmol) and [**1**]Cl_6 (41 mg, 0.045 mmol), **8a** was obtained as a yellow powder. Yield: 50 mg (quant.). ^{1}H-NMR (400 MHz, CD_3OD): δ (ppm) = 8.52 (br. s, 12H, *o*-Ar), 8.07 (s, 6H, *p*-Ar), 4.88 (s, 24H, NCH_2), 3.18 (s, 108H, $N(CH_3)_3$). $^{13}C\{^1H\}$-NMR (75 MHz, CD_3OD): δ (ppm) = 143.0 (s, Ar), 142.1 (s, Ar), 131.1 (m, overlapping *i*- and *o*-Ar), 68.4 (s, NCH_2), 53.6 (s, $N(CH_3)_3$). $^{31}P\{^1H\}$-NMR (162 MHz, CD_3OD): δ (ppm) = 24.5 (s, $^1J_{P,Pt}$ = 2655 Hz). ESI MS: (*m*/*z*) 658.62 {$[M\text{-}3Cl]^{3+}$, calc. 658.59}, 484.72 {$[M\text{-}4Cl]^{4+}$, calc. 484.70}. Elem. anal. found: C 48.36, H 7.30, Cl 23.46, N 8.04, P 2.89%. Calc. for $C_{84}H_{150}Cl_{14}N_{12}P_2Pt$ (2081.56): C 48.47, H 7.26, Cl 23.85, N 8.07, P 2.98%.

[$PtCl_2$(**2**)$_2$]Cl_{12} (8b)

Starting from $PtCl_2$(cod) (14 mg, 0.037 mmol) and [**2**]Cl_6 (0.10 g, 0.075 mmol), **8b** was obtained as a yellow powder. Yield: 0.12 g (quant.). ^{1}H-NMR (300 MHz, CD_3OD): δ (ppm) = 8.69 (br. s, 12H, *o*-Ar), 8.03 (s, 6H, *p*-Ar), 7.72 (d, $^3J_{H,H}$ = 7.8 Hz, 24H, *o*-Ph), 7.47 (m, 36H, *m*- and *p*-Ph), 4.93 (br. s, 24H, Ph-CH_2N), 4.75 (br. s, 24H, Bn-NCH_2), 2.96 (s, 72H, $N(CH_3)_2$). $^{13}C\{^1H\}$-NMR (100 MHz, CD_3OD): δ (ppm) = 143.0 (br. s, Ar), 142.4 (s, Ar), 134.6 (s, Ph), 132.0 (s, Ph), 130.8 (br. s, Ar), 130.3 (s, Ph), 129.5 (s, Ar), 129.0 (s, Ph), 67.0 (s, NCH_2), 66.6 (s, NCH_2), 49.7 (s, $N(CH_3)_2$). $^{31}P\{^1H\}$-NMR (122 MHz, CD_3OD): δ (ppm) = 24.8 (s, $^1J_{P,Pt}$ = 2663 Hz). HR-ESI MS: (*m*/*z*) 962.390 {$[M\text{-}3Cl]^{3+}$, calc. 962.385}, 713.046 {$[M\text{-}4Cl]^{4+}$, calc. 713.050}. Elem. anal. found: C 61.51, H 6.41, N 5.55, P 2.16%. Calc. for $C_{156}H_{198}Cl_{14}N_{12}P_2Pt$ (2994.73): C 62.57, H 6.66, N 5.61, P 2.07%.

$PtCl_2$(**4**)$_2$ (9b)

A solution of $PtCl_2$(cod) (33 mg, 0.089 mmol) in CH_2Cl_2 (3 mL) was added to a solution of **4** (189 mg, 0.178 mmol, 2.0 equiv.) in CH_2Cl_2 (10 mL). The mixture was heated at reflux temperature for 1 h and subsequently dried *in vacuo*, yielding **9b** as a viscous yellow oil (226 mg, quant.). ^{1}H-NMR (400 MHz, C_6D_6): δ (ppm) = (signals attributed to the *cis*-isomer) 7.80 (d, $^3J_{H,P}$ = 10.4 Hz, 12H, *o*-Ar), 7.67 (s, 6H, *p*-Ar), 7.32 (d, $^3J_{H,H}$ = 7.2 Hz, 12H, *o*-Ph), 7.20 (t, $^3J_{H,H}$ = 7.6 Hz, 12H, *m*-Ph), 7.08 (t, $^3J_{H,H}$ = 7.2 Hz, 6H, *p*-Ph), 3.27 (s, 12H, NCH_2), 3.23 (s, 12H, NCH_2), 1.96 (s, 18H, NCH_3). ^{13}C-NMR (100 MHz, C_6D_6): δ (ppm) = (signals attributed to the *cis*-isomer) 139.7 (br. s, Ar), 134.9 (br. s, Ar), 131.6 (s, Ar), 130.9 (s, Ar), 129.2 (s, Ph), 128.7 (s, Ph), 128.5 (s, Ph), 127.3 (s, Ph), 62.0 (s, NCH_2), 61.6 (s, NCH_2), 42.4 (s, NCH_3). $^{31}P\{^1H\}$-NMR (162 MHz, Toluene-d_8): δ (ppm) = 21.0 (s, $^1J_{P,Pt}$ = 2653 Hz, *trans*-isomer), 16.6 (s, $^1J_{P,Pt}$ = 3610 Hz, *cis*-isomer). MALDI-TOF MS: (*m*/*z*) 2350.9 {$[M\text{-}Cl]^+$, calc. 2351.2}. Elem. anal. found: C 72.49, H 6.90, N 6.95, P 2.54%. Calc. for $C_{144}H_{162}Cl_2N_{12}P_2Pt$ (2388.88): C 72.40, H 6.84, N 7.04, P 2.59%.

[PtI_2(**1**)$_2$]I_{12} (10a)

A solution of PtI_2(cod) (37 mg, 0.066 mmol) in CH_2Cl_2 (10 mL) was added at 60 °C to a solution of [**1**]I_6 (193 mg, 0.133 mmol, 2.0 equiv.) in MeOH (50 mL), upon which a precipitate formed. The mixture was heated at reflux temperature for 1 h and subsequently centrifuged. The precipitate was dried *in vacuo*, affording **10a** as a light yellow powder (179 mg, 81%). ^{1}H-NMR (400 MHz, D_2O): δ (ppm) = 8.53 (br. s, 12H, *o*-Ar), 7.99 (s, 6H, *p*-Ar), 4.89 (s, 24H, NCH_2), 3.24 (s, 108H, $N(CH_3)_3$). $^{13}C\{^1H\}$-NMR (75 MHz, D_2O): δ (ppm) = 142.0 (br. s, *m*-Ar), 141.2 (s, *p*-Ar), 134.1 (*pseudo* t, $J_{C,P}$ = 29.6 Hz, *i*-Ar), 129.5 (*pseudo* t, $J_{C,P}$ = 5.6 Hz, *o*-Ar), 67.5 (s, NCH_2), 53.4 (s, $N(CH_3)_3$). $^{31}P\{^1H\}$-NMR (162 MHz, D_2O): δ (ppm) = 16.4 (s, $^1J_{P,Pt}$ = 2583 Hz). ESI MS: (*m*/*z*) 993.46 {$[M\text{-}3I]^{3+}$, calc. 993.36}, 825.34 {$[M\text{-}$[**1**]$I_6\text{-}2I]^{2+}$, calc. 825.48}, 713.40 {$[M\text{-}4I]^{4+}$, calc. 713.29}, 545.43 {$[M\text{-}5I]^{5+}$, calc. 545.25}, 433.22 {$[M\text{-}6I]^{6+}$, calc. 433.23}. Elem. anal. found: C 29.76, H 4.78, I 52.39,

N 4.72, P 1.65, Pt 5.90%. Calc. for $C_{84}H_{150}I_{14}N_{12}P_2Pt$ (3361.89): C 30.01, H 4.50, I 52.85, N 5.00, P 1.84, Pt 5.80%.

[PtI$_2$(5)$_2$]I$_8$ (10b)

A solution of PtI$_2$(cod) (29 mg, 0.052 mmol) in CH_2Cl_2 (1 mL) was added at 60 °C to a solution of **[5]**I$_4$ (110 mg, 0.10 mmol, 2.0 equiv.) in MeOH (10 mL). The mixture was heated at reflux temperature for 1 h and subsequently dried *in vacuo*, affording **10b** as an orange powder (128 mg, quant.). ^{1}H-NMR (400 MHz, D_2O): δ (ppm) = 8.30 (t, $J_{H,P}$ = 5.0 Hz, *o*-Ar), 8.20 (m, 4H, *o*-Ph), 7.87 (s, 4H, *p*-Ar), 7.71 (m, 6H, *m*- and *p*-Ph), 4.75 (s, 16H, NCH_2), 3.15 (s, 72H, $N(CH_3)_3$). ^{13}C{^{1}H}-NMR (75 MHz, DMSO-d_6): δ (ppm) = (signals attributed to the *trans*-isomer) 139.9 (br. s, *m*-Ar), 139.1 (br. s, *p*-Ar), 137.6 (br. s, Ph), 135.7 (br. s, Ph), 134.3 (*pseudo* t, $J_{C,P}$ = 29.1 Hz, *i*-Ar), 131.4 (br. s, Ph), 129.7 (m, *i*-Ph), 128.5 (s, *o*-Ar), 65.8 (br. s, NCH_2), 51.8 (s, $N(CH_3)_3$). ^{31}P{^{1}H}-NMR (162 MHz, D_2O): δ (ppm) = 12.2 (s, $^1J_{P,Pt}$ = 2498 Hz). ESI MS: (*m*/*z*) 1379.6 {[M-**[5]**I$_4$–I]$^+$, calc. 1379.9}, 1155.3 {[M-2I]$^{2+}$, calc. 1155.5}, 728.26 {[M-3I]$^{3+}$, calc. 728.38}, 626.33 {[M-**[5]**I$_4$-2I]$^{2+}$, calc. 626.50}. Elem. anal. found: C 31.73, H 4.38, I 49.40, N 4.32, P 2.38, Pt 7.45%. Calc. for $C_{68}H_{110}I_{10}N_8P_2Pt$ (2565.75): C 31.83, H 4.32, I 49.46, N 4.37, P 2.41, Pt 7.60%.

[PtI$_2$(6)$_2$]I$_4$ (10c)

A solution of PtI$_2$(cod) (35 mg, 0.062 mmol) in CH_2Cl_2 (1 mL) was added at 60 °C to a solution of **[6]**I$_2$ (82 mg, 0.12 mmol, 2.0 equiv.) in MeOH (10 mL). The mixture was heated at reflux temperature for 1 h and subsequently dried *in vacuo*, affording **10c** as an orange powder (112 mg, quant.). ^{1}H-NMR (400 MHz, DMSO-d_6): δ (ppm) = (signals attributed to the *trans*-isomer) 7.88 (br. s, 8H, *o*-Ph), 7.74 (m, 6H, *o*- and *p*-Ar), 7.54 (s, 12H, *m*- and *p*-Ph), 4.67 (s, 8H, NCH_2), 3.00 (s, 36H, $N(CH_3)_3$). Minor signals attributed to the *cis*-isomer were observed at 4.44 (s, NCH_2) and 2.92 ppm (s, $N(CH_3)_3$); the aromatic signals were not resolved. ^{13}C{^{1}H}-NMR (100 MHz, DMSO-d_6): δ (ppm) = (signals attributed to the *trans*-isomer) 139.6 (s, Ar), 138.4 (s, Ar), 136.0 (*pseudo* t, $J_{C,P}$ = 29.1 Hz, *i*-Ar), 135.3 (s, Ph), 131.6 (s, Ar), 131.1 (s, Ph), 130.4 (*pseudo* t, $J_{C,P}$ = 29.9 Hz, *i*-Ph), 128.3 (s, Ph), 66.4 (s, NCH_2), 51.7 (s, $N(CH_3)_3$). ^{31}P{^{1}H}-NMR (121 MHz, DMSO-d_6): δ (ppm) = 12.4 (s, $^1J_{P,Pt}$ = 2478 Hz, *trans*-isomer), 11.8 (s, $^1J_{P,Pt}$ = 3471 Hz, *cis*-isomer). ESI MS: (*m*/*z*) 1642.2 {[M-I]$^+$, calc. 1642.0}, 981.60 {[M-**[6]**I$_2$–I]$^+$, calc. 981.93}, 756.82 {[M-2I]$^{2+}$, calc. 757.04}, 462.65 {[M-3I]$^{3+}$, calc. 462.73}. Elem. anal. found: C 35.12, H 3.92, I 43.11, N 3.22, P 3.45, Pt 11.10%. Calc. for $C_{52}H_{70}I_6N_4P_2Pt$ (1769.61): C 35.29, H 3.99, I 43.03, N 3.17, P 3.50, Pt 11.02%.

[PtI$_2$(7)$_2$]I$_6$ (11)

A solution of PtI$_2$(cod) (23 mg, 0.041 mmol) in CH_2Cl_2 (1 mL) was added at 60 °C to a solution of **[7]**I$_3$ (72 mg, 0.084 mmol, 2.0 equiv.) in MeOH (5 mL), upon which a precipitate formed. The mixture was heated at reflux temperature for 1 h. The precipitate was washed once with hot MeOH (5 mL) and subsequently dried *in vacuo*, affording **11** as a light orange powder (64 mg, 71%). ^{1}H-NMR (400 MHz, D_2O): δ (ppm) = 8.02 (m, *o*-Ar, *cis*-isomer), 7.81 (m, *o*-Ar, *trans*-isomer), 7.75 (d, $^3J_{H,H}$ = 8.4 Hz, *m*-Ar, *cis*-isomer), 7.59 (d, $^3J_{H,H}$ = 8.0 Hz, *m*-Ar, *trans*-isomer), 4.63, 4.62 (s, NCH_2, *cis* and *trans* isomers), 3.16, 3.15 (s, $N(CH_3)_3$, *cis* and *trans* isomers). ^{13}C{^{1}H}-NMR (100 MHz, D_2O, 65 °C): δ (ppm) = 136.5 (*pseudo* t, $J_{C,P}$ = 6.0 Hz, *m*-Ar, *trans*-isomer), 136.2 (*pseudo* t, $J_{C,P}$ = 5.4 Hz, *m*-Ar, *cis*-isomer), 134.4 (*pseudo* t, $J_{C,P}$ = 29.5 Hz, *i*-Ar, *trans*-isomer), 133.4 (*pseudo* t, $J_{C,P}$ = 5.6 Hz, *o*-Ar, *cis*-isomer), 133.2 (*pseudo* t, $J_{C,P}$ = 5.6 Hz, *o*-Ar, *trans*-isomer), 131.7 (s, *p*-Ar, *cis*-isomer), 131.2 (s, *p*-Ar, *trans*-isomer), 69.6 (s, NCH_2, *trans*-isomer), 69.3 (s, NCH_2, *cis*-isomer), 53.8 (s, $N(CH_3)_3$, *cis*-isomer), 53.7 (s, $N(CH_3)_3$, *trans*-isomer). The signal for *i*-Ar, *cis*-isomer was not resolved. ^{31}P{^{1}H}-NMR (162 MHz, D_2O): δ (ppm) = 12.0 (s, $^1J_{P,Pt}$ = 2467 Hz, *trans*-isomer), 11.2 (s, $^1J_{P,Pt}$ = 3491 Hz, *cis*-isomer). ESI MS: (*m*/*z*) 527.01 {[M-**[7]**I$_3$-2I]$^{2+}$, calc. 527.01}, 306.47 {[M-5I]$^{5+}$, calc. 306.47}, 234.38 {[M-6I]$^{6+}$, calc. 234.24}. Elem. anal. found: C 33.11, H 4.25, N 3.73, P 2.92, Pt 9.08%. Calc. for $C_{60}H_{90}I_8N_6P_2Pt$ (2167.68): C 33.25, H 4.18, N 3.88, P 2.86, Pt 9.00%.

X-Ray crystallography

All reflection intensities were measured using a Nonius KappaCCD diffractometer (equipped with a rotating anode) with graphite-monochromated Mo-Kα radiation (λ = 0.71073 Å) under the program COLLECT.[41] The program PEAKREF[42] was used to refine the cell dimensions. Data reduction was done using EVALCCD.[43] The structures of *trans*-**10a** and [PtI$_3$(**1**)]I$_5$ were, respectively, solved with the programs SHELXS-97[44] and DIRDIF08[45] and were both refined on F^2 with SHELXL-97.[44] Multi-scan semi-empirical absorption corrections (based on symmetry-related measurements) were applied to all data using the program SADABS.[46] The temperature of the data collection was controlled using the system OXFORD CRYOSTREAM 600 (manufactured by OXFORD CRYOSYSTEMS). H-atoms (except when specified) were placed at calculated positions and refined with a riding model (instructions AFIX 23, AFIX 43 and AFIX 137) with isotropic displacement parameters having values 1.2 or 1.5 times U_{eq} of the attached C atom. In the structure of [PtI$_3$**1**]I$_5$, the D-atoms (treated as hydrogen atoms in the model since the elements H and D have the same number of electrons and since no interpretable difference between H and D can be derived from X-ray diffraction measurements) of the two crystallographically independent lattice water molecules were located in difference Fourier maps and restrained using the DFIX instructions such that the O–H distances and H–O–H angles have reasonable values [*i.e.*, d(O–H) ≈ 0.84 Å, d(H···H) ≈ 1.33 Å so that H–O–H ≈ 104.5°]. Geometry calculations and graphical illustrations (displacement ellipsoid plots) were made with the PLATON program.[47]

Refinement details for *trans*-10a. The asymmetric unit of *trans*-**10a** contains one half of the *trans*-**10a** complex [the Pt(II) centre is found at sites of inversion symmetry, the other half of *trans*-**10a** complex is symmetry generated], four ordered lattice iodides with full occupancy (I2, I3, I4, I5), one ordered lattice iodide with a population factor of 0.5 (I7), one fully-occupied lattice iodide ion disordered over two positions [I6A/I6B, major occupancy factor = 0.534(2)], one half-occupied lattice iodide ion disordered over two positions [I8A/I8B, major occupancy factor = 0.327(3) × 0.5] and some unresolved chemical species (probably some disordered solvent molecules). The contribution of these species was subsequently taken out for the final stage of the refinement using the program SQUEEZE (see details below).[48]

Crystallographic data for *trans*-10a. $C_{84}H_{150}I_{14}N_{12}P_2Pt$ + solvent, FW = 3361.79,‡ needle, 0.48 × 0.15 × 0.12 mm^3, triclinic, $P\bar{1}$ (no. 2), a = 14.5266(2), b = 16.8586(1), c = 17.1335(2) Å, α = 101.202(1), β = 103.197(1), γ = 113.487(1)°, V = 3550.37(8) Å^3, Z = 1, D_x = 1.57 g cm^{-3},‡ μ = 4.09 mm^{-1}.‡ 52744 reflections were measured up to a resolution of (sin $\theta/\lambda)_{max}$ = 0.65 Å^{-1}. 16172 reflections were unique (R_{int} = 0.030), of which 13846 were observed [$I > 2\sigma(I)$]. 558 parameters were refined. R_1/wR_2 [$I > 2\sigma(I)$]: 0.0394/0.1132. R_1/wR_2 [all refl.]: 0.0466/0.1172. S = 1.104. Residual electron density found between −1.93 and 2.77 eÅ^{-3}. SQUEEZE details: one void of 284 Å^3 filled with 94 electrons and two voids of 215 Å^3 filled with 72 electrons (all numbers are given per unit cell).

Refinement details for [PtI$_3$(1)]I$_5$. The asymmetric unit of [PtI$_3$(**1**)]I$_5$ contains one [PtI$_3$(**1**)]$^{5+}$ complex, two lattice deuterated water molecules and five lattice iodide counter anions. The lattice water molecules and some lattice iodide ions (I4, I5 and I8) form weak hydrogen bond O–H · · · I interactions (O · · · I ≈ 3.49–3.55 Å). The lattice iodide I7 is found at sites of twofold axial symmetry and the SHELX population was constrained to be 0.5. The occupancy factors of the remaining iodides I4, I5, I6, I8 and I9 were refined using the FVAR (free variable) instructions. The sum of these occupancy factors were constrained to be 4.5 using the SUMP instruction as a requirement for charge balance. The free variables for the occupancy factors of I4, I5, I6, I8 and I9 refined to 0.998(2), 0.997(2), 0.991(2), 0.972(2) and 0.541(2), respectively. The final difference Fourier map is relatively flat except for some peaks found near I9 (2.2–3.6 Å), which are as large as 3.3–4.1 e Å^{-3}. Such large peaks may result from disorder of the iodide I9 although there is no sign of disorder in its atomic displacement parameters, or may result from very disordered solvent molecules which may be partially contained in one void [(0.5, 0.171, 0.25)] found near I9.

Crystallographic data for [PtI$_3$(1)]I$_5$. $C_{42}H_{79}I_8N_6O_2PPt$, FW = 1941.37, plate, 0.24 × 0.18 × 0.06 mm^3, monoclinic, $C2/c$ (no. 15), a = 17.2539(5), b = 17.4111(5), c = 41.5254(9) Å, β = 90.2090(10), V = 12474.5(6) Å^3, Z = 8, D_x = 2.07 g cm^{-3}, μ = 6.27 mm^{-1}. 67316 reflections were measured up to a resolution of (sin $\theta/\lambda)_{max}$ = 0.59 Å^{-1}. 10730 reflections were unique (R_{int} = 0.044), of which 9090 were observed [$I > 2\sigma(I)$]. 581 parameters were refined. R_1/wR_2 [$I > 2\sigma(I)$]: 0.0369/0.0813. R_1/wR_2 [all refl.]: 0.0499/0.0862. S = 1.085. Residual electron density found between −1.15 and 4.07 eÅ^{-3}.

Acknowledgements

The authors thank Cees Versluis and Ronald van Ooijen (Bijvoet Institute, Biomolecular Mass Spectrometry, Utrecht University) for the ESI-MS analyses.

Notes and references

1 (*a*) D. J. M. Snelders, G. van Koten and R. J. M. Klein Gebbink, *Chem. Eur. J.*, 2011, **17**, 42–57; (*b*) P. W. N. M. Van Leeuwen (Editor), *Supramolecular Catalysis*, Wiley-VCH, Weinheim, 2008.
2 (*a*) Reviews: M. J. Wilkinson, P. W. N. M. Van Leeuwen and J. N. H. Reek, *Org. Biomol. Chem.*, 2005, **3**, 2371–2383; (*b*) B. Breit, *Angew. Chem., Int. Ed.*, 2005, **44**, 6816–6825; (*c*) A. J. Sandee and J. N. H. Reek, *Dalton Trans.*, 2006, 3385–3391.
3 Some recent examples: (*a*) C. Machut, J. Patrigeon, S. Tilloy, H. Bricout, F. Hapiot and E. Monflier, *Angew. Chem., Int. Ed.*, 2007, **46**, 3040–3042; (*b*) A. C. Laungani, J. M. Slattery, I. Krossing and B. Breit, *Chem.–Eur. J.*, 2008, **14**, 4488–4502; (*c*) F. W. Patureau, M. Kuil, A. J. Sandee and J. N. H. Reek, *Angew. Chem., Int. Ed.*, 2008, **47**, 3180–3183 and references therein; (*d*) C. G. Oliveri, P. A. Ulmann, M. J. Wiester and C. A. Mirkin, *Acc. Chem. Res.*, 2008, **41**, 1618–1629; (*e*) S. A. Moteki and J. M. Takacs, *Angew. Chem., Int. Ed.*, 2008, **47**, 894–897.
4 (*a*) P. A. Duckmanton, A. J. Blake and J. B. Love, *Inorg. Chem.*, 2005, **44**, 7708–7710; (*b*) L. A. Knight, Z. Freixa, P. W. N. M. Van Leeuwen and J. N. J. Reek, *Organometallics*, 2006, **25**, 954–960; (*c*) Z. Freixa and P. W. N. M. Van Leeuwen, *Coord. Chem. Rev.*, 2008, **252**, 1755–1786.
5 H. Gulyás, J. Benet-Buchholz, E. C. Escudero-Adan, Z. Freixa and P. W. N. M. Van Leeuwen, *Chem.–Eur. J.*, 2007, **13**, 3424–3430.
6 (*a*) B. Cornils and E. G. Kuntz, *J. Organomet. Chem.*, 1995, **502**, 177–186; (*b*) O. Herd, D. Hoff, K. W. Kottsieper, C. Liek, K. Wenz, O. Stelzer and W. S. Sheldrick, *Inorg. Chem.*, 2002, **41**, 5034–5042; (*c*) E. Genin, R. Amengual, V. Michelet, M. Savignac, A. Jutand, L. Neuville and J. P. Genêt, *Adv. Synth. Catal.*, 2004, **346**, 1733–1741; (*d*) L. R. Moore, E. C. Western, R. Craciun, J. M. Spruell, D. A. Dixon, K. P. O'Halloran and K. H. Shaughnessy, *Organometallics*, 2008, **27**, 576–593.
7 (*a*) R. T. Smith and M. C. Baird, *Inorg. Chim. Acta*, 1982, **62**, 135–139; (*b*) E. Renaud, R. B. Russell, S. Fortier, S. J. Brown and M. C. Baird, *J. Organomet. Chem.*, 1991, **419**, 403–415; (*c*) T. Okano, N. Harada and J. Kiji, *Chem. Lett.*, 1994, 1057–1060; (*d*) B. Mohr, D. M. Lynn and R. H. Grubbs, *Organometallics*, 1996, **15**, 4317–4325; (*e*) A. Hessler and O. Stelzer, *J. Org. Chem.*, 1997, **62**, 2362–2369; (*f*) F. P. Pruchnik and P. Smolenski, *Appl. Organomet. Chem.*, 1999, **13**, 829–836; (*g*) C. C. Brasse, U. Englert and A. Salzer, *Organometallics*, 2000, **19**, 3818–3823; (*h*) R. B. DeVasher, L. R. Moore and K. H. Shaughnessy, *J. Org. Chem.*, 2004, **69**, 7919–7927; (*i*) M. P. Coles and P. B. Hitchcock, *Chem. Commun.*, 2007, 5229–5231.
8 (*a*) Reviews: W. A. Herrmann and C. W. Kohlpaintner, *Angew. Chem., Int. Ed. Engl.*, 1993, **32**, 1524–1544; (*b*) O. Stelzer, S. Rossenbach, D. Hoff, M. Schreuder-Goedheijt, P. C. J. Kamer, J. N. H. Reek and P. W. N. M. Van Leeuwen, *Multiphase homogeneous catalysis*, Wiley-VCH, 2005, **1**, 66-82; (*c*) K. H. Shaughnessy, *Eur. J. Org. Chem.*, 2006, 1827–1835; (*d*) D. M. Chisholm and J. S. McIndoe, *Dalton Trans.*, 2008, 3933–3945; (*e*) K. H. Shaughnessy, *Chem. Rev.*, 2009, **109**, 643–710.
9 (*a*) R. Kreiter, R. J. M. Klein Gebbink and G. van Koten, *Tetrahedron*, 2003, **59**, 3989–3997; (*b*) D. J. M. Snelders, R. Kreiter, J. J. Firet, G. van Koten and R. J. M. Klein Gebbink, *Adv. Synth. Catal.*, 2008, **350**, 262–266; (*c*) D. J. M. Snelders, G. van Koten and R. J. M. Klein Gebbink, *J. Am. Chem. Soc.*, 2009, **131**, 11407–11416; (*d*) D. J. M. Snelders, C. Van Der Burg, M. Lutz, A. L. Spek, G. van Koten and R. J. M. Klein Gebbink, *ChemCatChem*, 2010, **2**, 1425–1437; (*e*) D. J. M. Snelders, K. Kunna, C. Müller, D. Vogt, G. van Koten and R. J. M. Klein Gebbink, *Tetrahedron: Asymmetry*, 2010, **21**, 1411–1420.
10 I. M. Al-najjar, *Inorg. Chim. Acta*, 1987, **128**, 93–104.
11 (*a*) A. W. Kleij, R. van de Coevering, R. J. M. Klein Gebbink, A. Noordman, A. L. Spek and G. van Koten, *Chem.–Eur. J.*, 2001, **7**, 181–191; (*b*) R. van de Coevering, P. C. A. Bruijnincx, M. Lutz, A. L. Spek, G. van Koten and R. J. M. Klein Gebbink, *New J. Chem.*, 2007, **31**, 1337–1348.
12 Isomerization of square planar Pt(II) complexes is catalyzed by free phosphine: see ref. 29.
13 No other peak appeared, indicating that these species had irreversibly converted to *trans*-**8a** and *trans*-**8b**, respectively. When *trans*-**8a** was synthesized starting from PtCl$_2$(DMSO)$_2$ as the Pt precursor, this minor product did not form, indicating that it is a thermally labile intermediate species in the reactions of these phosphines with PtCl$_2$(cod).
14 R. Kreiter, J. J. Firet, M. J. J. Ruts, M. Lutz, A. L. Spek, R. J. M. Klein Gebbink and G. van Koten, *J. Organomet. Chem.*, 2006, **691**, 422–432.
15 When a solution of **9b** in toluene-d$_8$ was heated in the presence of a small quantity of free **4**, the *cis*-*trans* equilibrium shifted in favour of the *trans*-isomer. Isomerization occurred at temperatures higher than 65 °C. At 105 °C, the *cis* : *trans* ratio had shifted from 85 : 15 to 55 : 45. After cooling, the original product distribution was restored. No isomerization occurred in the absence of free **4**.
16 The reaction of PtCl$_2$(DMSO)$_2$ with one equiv. of PPh$_3$ in CDCl$_3$ was also performed; a mixture of *cis*- and *trans*-PtCl$_2$(PPh$_3$)$_2$ and *cis*-PtCl$_2$(DMSO)(PPh$_3$) was obtained (approximate ratio: 3 : 4 : 3). The complex *cis*-PtCl$_2$(DMSO)(PPh$_3$) was identified by a characteristic

‡ excluding the unresolved entity contribution.

ν(S=O) frequency in the IR spectrum at 1154 cm^{-1}, as well as a resonance in the ^{1}H-NMR spectrum at 3.30 ppm with Pt satellites ($^3J_{H,Pt}$ = 20 Hz). These spectroscopic data are in agreement with the literature and indicate that the DMSO is bonded as a ligand to the Pt(II) centre and that coordination occurs through the S atom, rather than the O atom; see ref. 17.

17 (*a*) J. H. Price, A. N. Williamson, R. F. Schramm and B. B. Wayland, *Inorg. Chem.*, 1972, **11**, 1280–1284; (*b*) J. A. Davies, C. S. Hasselkus, C. N. Scimar, A. Sood and V. Uma, *J. Chem. Soc., Dalton Trans.*, 1985, 209–211; (*c*) J. A. Davies and A. Sood, *Inorg. Chem.*, 1985, **24**, 4213–4214.

18 B. Schmid, L. M. Venanzi, A. Albinati and F. Mathey, *Inorg. Chem.*, 1991, **30**, 4693–4669.

19 The purity of the employed batch of ligand [**1**][BF_4]$_6$ was confirmed by elemental analysis (see Ref. 9e), excluding the possibility that some [$PtCl_3$(**1**)]Cl_5 was formed simply due to residual chloride in the batch of ligand [**1**][BF_4]$_6$.

20 (*a*) J. Fresneda, E. De Jesus, P. Gómez-Sal and C. López Mardomingo, *Eur. J. Inorg. Chem.*, 2005, 1468–1476; (*b*) R. J. Topping, L. D. Quin and A. L. Crumbliss, *J. Organomet. Chem.*, 1990, **385**, 131–145.

21 In the case of complex **10c**, the hydrophobic interactions between the unsubstituted phenyl groups are likely to be important. These interactions should be stronger in D_2O compared to DMSO-d_6, and could explain the reversed *cis*-*trans* preference for **10c** in these solvents.

22 During these measurements, no free phosphine was present, suggesting that the isomerization is catalyzed by free iodide: W. J. Louw, *Inorg. Chem.*, 1977, **16**, 2147. In contrast to **11**, the *cis*- and *trans*-isomers of complexes **10b** and **10c** did not significantly interconvert upon increasing the temperature, not even in the presence of free [**5**]I_4 and [**6**]I_2, respectively.

23 T. E. Müller and D. M. P. Mingos, *Transition Met. Chem.*, 1995, **20**, 533–539.

24 Measuring a ^{31}P-NMR spectrum in DMSO-d_6 of the product of this reaction gave identical spectral data for [PtI_3**1**]I_5 as was observed by dissolving *trans*-**10a** in DMSO-d_6.

25 O. F. Wendt and L. I. Elding, *J. Chem. Soc., Dalton Trans.*, 1997, 4725–4731.

26 (*a*) N. M. Boag, K. Mohan Rao and N. J. Terrill, *Acta Crystallogr., Sect. C: Cryst. Struct. Commun.*, 1991, **C47**, 1064–1065; (*b*) E. C. Alyea, S. A. Dias, G. Ferguson and P. J. Roberts, *J. Chem. Soc., Dalton Trans.*, 1979, 948–951; (*c*) N. W. Alcock and P. G. Leviston, *J. Chem. Soc., Dalton Trans.*, 1974, 1834–1836.

27 Y. Marcus and G. Hefter, *Chem. Rev.*, 2006, **106**, 4585–4621.

28 (*a*) J. Chatt and R. G. Wilkins, *J. Chem. Soc.*, 1952, 273–278; (*b*) J. N. Harvey, K. M. Heslop, A. G. Orpen and P. G. Pringle, *Chem. Commun.*, 2003, 278–279.

29 G. K. Anderson and R. J. Cross, *Chem. Soc. Rev.*, 1980, **9**, 185–215.

30 T. G. Appleton, H. C. Clark and L. E. Manzer, *Coord. Chem. Rev.*, 1973, **10**, 335–422.

31 C. A. Tolman, *Chem. Rev.*, 1977, **77**, 313–348.

32 A. J. Cheney, B. E. Mann, B. L. Shaw and R. M. Slade, *J. Chem. Soc. A*, 1971, 3833–3842.

33 Addition of salts is known to increase solvent polarity. See, for example: M. C. Rezende, *Tetrahedron*, 1988, **44**, 3513–3522.

34 B. A. Harper, D. A. Knight, C. George, S. L. Brandow, W. J. Dressick, C. S. Dalcey and T. L. Schull, *Inorg. Chem.*, 2003, **42**, 516–524.

35 A. Hessler, S. Kucken, O. Stelzer, J. Blotevogel-Baltronat and W. S. Sheldrick, *J. Organomet. Chem.*, 1995, **501**, 293–302.

36 L. W. Francisco, D. A. Moreno and J. D. Atwood, *Organometallics*, 2001, **20**, 4237–4245.

37 G. Wilkinson, *Comprehensive Coordination Chemistry, 1st ed.*, 1987, **1**, 311–329.

38 In complexes of the type $PtCl_2$(DMSO)(L), the phosphine ligand and the DMSO ligand usually adopt a *cis* orientation; see ref. 17 The $^1J_{P,Pt}$ coupling constants in ^{31}P-NMR observed for the complexes [$PtCl_2$(DMSO-d_6)(L)][BF_4]$_6$ (L = **1**, **2**) indicate that this is indeed the case.

39 D. Drew, J. R. Doyl and A. G. Shaver, *Inorg. Synth.*, 1972, **13**, 47.

40 H. C. Clark and L. E. Manzer, *J. Organomet. Chem.*, 1973, **59**, 411–428.

41 Nonius. COLLECT; Nonius BV, Delft, The Netherlands, 1999.

42 A. M. M. Schreurs, *PEAKREF*, University of Utrecht, The Netherlands, 2005.

43 A. J. M. Duisenberg, L. M. J. Kroon-Batenburg and A. M. M. Schreurs, *J. Appl. Crystallogr.*, 2003, **36**, 220–229.

44 G. M. Sheldrick, *Acta Crystallogr., Sect. A*, 2008, **64**, 112.

45 P. T. Beurskens, G. Beurskens, R. de Gelder, S. Garcia-Granda, R. O. Gould and J. M. M. Smits, *The DIRDIF 2008 program system*, Crystallography Laboratory, University of Nijmegen, The Netherlands, 2008.

46 G. M. Sheldrick, *SADABS, Version 2006/1*, University of Göttingen, Germany, 2006.

47 A. L. Spek, *J. Appl. Crystallogr.*, 2003, **36**, 7–13.

48 P. van der Sluis and A. L. Spek, *Acta Crystallogr., Sect. A: Found. Crystallogr.*, 1990, **46**, 194–201.

